

**Tatiana Clemente Pires**

Degree in Biochemistry

## Exploring malate:quinone oxidoreductases – MQO

Dissertation to obtain the Master degree in Biochemistry for Health

Supervisor: Manuela M. Pereira, FCUL

**September, 2019**



**Tatiana Clemente Pires**

## Exploring malate:quinone oxidoreductases – MQO

Dissertation to obtain the Master degree in Biochemistry for Health

Supervisor: Manuela M. Pereira, FCUL

Jury:

President: Pedro Matias, ITQB NOVA  
Opponent: Margarida Archer, ITQB NOVA  
Member: Teresa Catarino, FCT NOVA

**Instituto de Tecnologia Química e Biológica, António Xavier**

**September, 2019**



## Exploring malate:quinone oxidoreductases – MQO

### ***Copyright***

O Instituto de Tecnologia Química e Biológica António Xavier e a Universidade Nova de Lisboa têm o direito, perpétuo e sem limites geográficos, de arquivar e publicar esta dissertação através de exemplares impressos reproduzidos em papel ou de forma digital, ou por qualquer outro meio conhecido ou que venha a ser inventado, e de a divulgar através de repositórios científicos e de admitir a sua cópia e distribuição com objetivos educacionais ou de investigação, não comerciais, desde que seja dado crédito ao autor e editor.



## Agradecimentos

Em primeiro lugar, à minha orientadora Doutora Manuela Pereira por quem tenho uma grande admiração e a quem quero agradecer a oportunidade de desenvolver o meu projeto no seu grupo de investigação. Por me ter acompanhado, transmitido conhecimento e ajudado ao longo deste ano. Estou muito grata pela experiência enriquecedora que me proporcionou.

Ao longo deste ano, tive a possibilidade de trabalhar com pessoas incríveis que me ajudaram bastante e me ensinaram ainda mais. A todos os elementos do Grupo *Biological Energy Transduction*, deixo o meu profundo agradecimento. À Patrícia Refojo pelo conhecimento transmitido e pela ajuda nos momentos de dúvida. Ao Filipe por ser uma pessoa com um espírito crítico incrível que tantas vezes me auxiliou e fez ver que estava errada e por me fazer perceber que a nossa opinião deve ser expressada de forma fundamentada. À Diana, que mesmo chegando já no fim deste projeto, me aconselhou e encorajou bastantes vezes. À Patrícia Pires por me ter acompanhado ao longo deste ano e me entender completamente uma vez que abraçou a dissertação de mestrado ao mesmo tempo que eu. Por fim, a pessoa que foi mais importante neste projeto, à Filipa Sena. A Filipa foi a pessoa que me apoiou a mil por cento ao longo deste ano, foi quem exigiu tudo de mim e ao mesmo tempo se preocupou comigo, foi quem me ensinou como devia fazer, advertiu para como não devia fazer e foi quem nunca me deixou fazer absolutamente nada sem saber o seu propósito, despertando o meu espírito crítico. Foi uma co-orientadora sem o ser, foi uma professora sendo aluna de doutoramento, foi uma amiga sendo uma colega de laboratório. Um obrigado não chega para agradecer tudo o que foste para mim e que tenho a certeza de que vais continuar a ser.

Ao ITQB, à FCUL e às respetivas unidades de investigação, MOSTMICRO e BioISI, por proporcionarem as condições necessárias para que fosse possível desenvolver este projeto de investigação. Quero agradecer a todos os colaboradores de ambas as instituições que de alguma forma também foram intervenientes neste projeto, mas em especial ao fantástico João Carita por estar sempre ocupado, mas ao mesmo tempo sempre disponível para me ajudar.

À professora Helena Gaspar por se disponibilizar e ajudar no âmbito das experiências realizadas no HPLC e ao professor Rodrigo Almeida por para além de disponibilizar o espectrofluorímetro, auxiliar sempre que foi necessário.

Quero ainda agradecer ao Professor Miguel Teixeira, como responsável da *Metalloproteins and Bioenergetics Unit* e aos elementos desta unidade por nunca me terem negado ajuda quando precisei.

À professora Teresa Catarino por ter despertado em mim o gosto pela enzimologia, ainda durante a licenciatura, premindo o gatilho para o início do meu projeto neste grupo de investigação. Reconheço na professora Teresa um exemplo de dedicação e preocupação para com os seus alunos, algo que não foi muito comum durante o meu percurso académico, o que me faz estar grata por ter tido a oportunidade de a conhecer.

À minha família pela compreensão relativamente à minha ausência ao longo deste ano, pelo apoio, pela força para continuar e por de uma maneira ou de outra estar sempre presente quando eu precisei.

Aos meus amigos tenho de agradecer pelos momentos de distração que permitiram que me distanciasse o suficiente do trabalho de modo a relaxar e voltar ao trabalho com outra energia, por me darem força para não desistir e por me compreenderem. Um agradecimento especial à Jéssica, a amiga que me acompanhou de perto e que apesar de todos os seus problemas esteve sempre disponível para mim.

Ao meu pai que é um exemplo de pessoa trabalhadora, que me ensinou que não se atingem objetivos a dormir até ao meio dia, mas sim a levantar e encontrar caminhos que nos levem onde queremos chegar.

Ao meu namorado, o Tiago, um agradecimento por todas as palavras de incentivo, por todo o apoio nos momentos de maior aperto, por nunca me ter deixado sozinha, por ter feito e continuar a fazer tudo para me ver feliz, por me mostrar que a vida não pode ser tão séria e por todo o carinho.

Ao pilar da minha vida, à minha mãe, à pessoa que me fez ser quem eu sou hoje, que é um exemplo de esforço, dedicação e persistência, que representa o mundo para mim, que permitiu que a minha formação chegasse a este ponto e que nunca se negou a nada para me ver feliz. À pessoa que representa aquilo que eu um dia quero ser, eu quero agradecer por tudo o que fez e continua a fazer por mim mesmo quando eu não retribuo da melhor forma.

Por fim, obrigada avó, sei que apesar da tua partida me ter feito ir abaixo, tu estás aí em cima a olhar por mim e que foste tu que me deste a força necessária para concluir este projeto.

“Estás tão bonita hoje...”



## **Resumo**

As malato:quinona oxidoreductases (MQOs) são proteínas que estão associadas à membrana, catalisando a oxidação malato a oxaloacetato e a redução de quinona a quinol. As MQOs são consideradas proteínas com um papel importante no metabolismo dos organismos, integrando o ciclo dos ácidos tricarboxílicos, a cadeia respiratória e em alguns casos podem ainda fazer parte de outras vias metabólicas como o ciclo do fumarato.

As MQOs encontram-se distribuídas nos três domínios da vida e para este estudo selecionaram-se MQOs de *Staphylococcus aureus*, *Escherichia coli*, *Helicobacter pylori* e *Plasmodium falciparum* devido à natureza patogénica destes organismos, que representa uma ameaça para a saúde pública.

Surpreendentemente, considerando o papel central destas proteínas no metabolismo energético dos organismos, não existe muita informação relativa à relação estrutura-função das MQOs. Assim este estudo teve como objetivo caracterizar bioquímica e funcionalmente estas proteínas. Foram realizados testes para determinar as melhores condições para a expressão de MQOs. As MQO 1 e MQO 2 de *S. aureus* e a MQO de *E. coli* foram purificadas com sucesso. A caracterização bioquímica realizada à MQO 1 de *S. aureus* incluiu a determinação do grupo prostético por HPLC e a identificação da proteína por espetrometria de massa. Foram ainda realizados ensaios de cinética de estado estacionário visando a investigação do mecanismo catalítico e estudos de interação proteína-substrato utilizando espectroscopia de fluorescência para obter parâmetros de interação e investigar os efeitos desta interação. Os resultados obtidos revelaram que a interação do inibidor, HQNO, com a proteína é diferente da do oxaloacetato e da menaquinona (DMN). Para além disto, a MQO 1 de *S. aureus* mostrou ter o comportamento característico de Michaelis-Menten para os dois substratos e a sua atividade enzimática é afetada pela presença de HQNO. Observámos ainda que a MQO de *E. coli* prefere utilizar ubiquinona em vez de menaquinona.

**Palavras-chave:** proteínas monotópicas; malato; quinonas; estudos de inibição; interação proteína-ligando.



## **Abstract**

Malate:quinone oxidoreductases (MQOs) are membrane-bound proteins that catalyze the oxidation of malate to oxaloacetate and the reduction of the quinone to quinol. MQOs are considered proteins with a central role in the metabolism of the organisms, because they include the Tricarboxylic Acid Cycle, the respiratory chain and in some cases MQOs can also be part of other pathways, like the fumarate cycle.

MQOs are present in the three domains of life, and for this study MQOs from *Staphylococcus aureus*, *Escherichia coli*, *Helicobacter pylori* and *Plasmodium falciparum* were selected due to the organisms' pathogenic nature, which represents a threat to human health.

Surprisingly, considering the central role of these proteins in the energetic metabolism of the organisms, there is little information about the structure-function relationship in MQOs. In this study we aimed at biochemically and functionally characterizing these proteins. For this, tests were performed to determine the best conditions for the expression of MQOs. MQO 1 and MQO 2 from *S. aureus* and MQO from *E. coli* were successfully purified. Biochemical characterization including determination of the prosthetic group by HPLC and identification of the protein by mass spectrometry was achieved for MQO 1 from *S. aureus*. Moreover, steady-state kinetics assays were done to explore the catalytic mechanism of these enzymes and protein-substrate binding studies were performed using fluorescence spectroscopy to obtain binding parameters and investigate the effects of the interaction of the substrates with MQO at the protein level. Our combined results revealed that the inhibitor, HQNO, interacts with the protein in a different way from those of oxaloacetate or menaquinone (DMN). In addition, MQO 1 from *S. aureus* showed a Michaelis-Menten behavior towards both substrates and its enzymatic activity is affected by the presence of HQNO. We observed that MQO from *E. coli* preferably uses ubiquinone rather than menaquinone.

**Keywords:** monotopic proteins; malate; quinones; inhibition studies; protein-ligand interaction.



## **Table of contents**

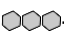
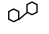
1.	Introduction.....	1
1.1.	Energetic metabolism .....	1
1.2.	The role of Malate:quinone oxidoreductases in metabolism .....	1
1.2.1.	Tricarboxylic Acid Cycle as a central metabolic pathway .....	2
1.2.2.	Respiratory chain.....	3
1.2.3.	Other metabolic pathways .....	4
1.3.	Malate:quinone oxidoreductases.....	5
1.3.1.	MQOs in pathogenic organisms .....	5
1.3.1.1.	<i>Staphylococcus aureus</i> .....	6
1.3.1.2.	<i>Escherichia coli</i> .....	6
1.3.1.3.	<i>Helicobacter pylori</i> .....	6
1.3.1.4.	<i>Plasmodium falciparum</i> .....	7
2.	Objectives .....	9
3.	Materials and Methods .....	11
3.1.	Expression Tests .....	11
3.2.	Cell growth.....	12
3.2.1.	MQO 1 and MQO 2 from <i>Staphylococcus aureus</i> .....	12
3.2.2.	MQO from <i>Escherichia coli</i> .....	13
3.3.	Protein Purification .....	13
3.4.	Protein quantification .....	14
3.5.	Mass Spectrometry.....	14
3.6.	Identification of the flavin prosthetic group .....	14
3.7.	Determination of the oligomerization state .....	15
3.8.	Catalytic activity assays.....	15
3.9.	UV-Visible Spectroscopy .....	15
3.10.	Steady-state Kinetic Assays .....	15
3.11.	Inhibition Assays.....	16
3.12.	Fluorescence substrate binding studies .....	16
4.	Results and Discussion .....	19
4.1.	Biochemical characterization.....	19

4.1.1.	Expression of MQOs .....	19
4.1.2.	Purification of MQO 1 and MQO 2 from <i>S. aureus</i> and MQO from <i>E. coli</i> .....	21
4.1.2.1.	MQO 1 from <i>S. aureus</i> .....	21
4.1.2.2.	MQO 2 from <i>S. aureus</i> .....	23
4.1.2.3.	MQO from <i>E. coli</i> .....	26
4.1.3.	Protein quantification .....	29
4.1.4.	Protein identification .....	30
4.1.5.	Identification of the flavin prosthetic group .....	30
4.1.6.	Oligomerization state of MQO .....	31
4.2.	Functional Characterization.....	32
4.2.1.	Catalytic activity assays.....	32
4.2.2.	Enzymatic activity pH profile.....	33
4.2.3.	Reduction of MQO .....	34
4.2.4.	Steady-state Kinetic Assays .....	35
4.2.5.	Inhibition assays .....	37
4.2.6.	Fluorescence substrate binding studies .....	39
5.	Conclusion .....	43
6.	References .....	45
7.	Appendix.....	49

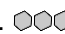
## **Table of contents of figures**

**Figure 1.1-** Schematic representation of metabolic pathways. Metabolic pathways converging in the Tricarboxylic Acid Cycle. Adapted from<sup>10</sup>. ..... 2

**Figure 1.2-** Representation of the canonical/mitochondrial respiratory chain. Four complexes are present in this respiratory chain and the arrangement of the complexes as proposed to date is represented. (+) and (-) indicate the positive and negative sides of the transmembrane difference in the electrochemical potential, respectively. .... 3

**Figure 1.3-** Schematic representation of X:quinone oxidoreductases present in the respiratory chain of *Staphylococcus aureus*.  - Representation of the flavin.  - Representation of the thiamine diphosphate (TPP). (+) and (-) indicates the positive and negative sides of the transmembrane difference in the electrochemical potential, respectively. Adapted from<sup>16</sup>. .... 4

**Figure 1.4-** Representation of the Fumarate cycle in *Plasmodium falciparum*. Enzymes involved in the Fumarate cycle: I- Adenylosuccinate synthetase; II- Adenylosuccinate lyase; III- Adenosine monophosphate deaminase; IV- Fumarate hydratase; V- Malate:quinone oxidoreductase; VI- Aspartate aminotransferase. Substrates of the Purine salvage pathway: IMP- Inosine monophosphate; SAMP- Adenylosuccinate; AMP- Adenosine monophosphate<sup>18</sup>. .... 4

**Figure 1.5-** Representation of malate:quinone oxidoreductases.  - Representation of the flavin. (+) and (-) indicates the positive and negative sides of the transmembrane difference in the electrochemical potential, respectively. Adapted from<sup>16</sup>. .... 5

**Figure 1.6-** Quinones chemical structure. A- Structure of Ubiquinone analog (DDB); B- Structure of Menaquinone analog (DMN). .... 6

**Figure 3.1-** Chemical structures of malate (A) and oxaloacetate (B). .... 17

**Figure 4.1-** SDS-PAGE gels of broken cells expressing genes coding for different MQOs. SDS-PAGE gel: Stacking and Resolving Gel – 15 % acrylamide. **A-** MQO 1 from *S. aureus* (molecular mass ~ 57 kDa); **B-** MQO 2 from *S. aureus* (molecular mass ~ 55 kDa); **C-** MQO from *E. coli* (molecular mass ~ 60 kDa); **D-** MQO from *H. pylori* (molecular mass ~ 50.6 kDa); Lane 1: Cells before induction with 1 mM of IPTG; Lane 2: Broken cells 4 hours after induction; Lane 3: Cells 16 hours after induction; M- PeqGold protein marker (**A**, **B** and **D**) or Low molecular weight (LMW) protein marker (**C**). Red boxes indicate the regions of the protein bands corresponding to the sizes of each MQO. .... 20

**Figure 4.2-** Expression of three genes coding for MQOs during large scale growths. SDS-PAGE gel: Stacking and Resolving Gel – 15 % acrylamide. **A-** MQO 1 from *S. aureus* (molecular mass ~ 57 kDa); **B-** MQO 2 from *S. aureus* (molecular mass ~ 55 kDa); **C-** MQO from *E. coli* (molecular mass ~ 60 kDa). Lane 1: Broken cells before induction with 1 mM of IPTG; Lane 2: Broken cells 4 hours after induction; M- PeqGold protein marker. Red boxes indicate the regions of the protein bands corresponding to the sizes of each MQO. .... 21

**Figure 4.3-** SDS-PAGE gel of samples from all the steps in the purification of MQO 1 from *S. aureus*. SDS-PAGE gel: Stacking and Resolving gel – 15 % acrylamide. Molecular mass of MQO 1 (*S. aureus*): ~ 57 kDa. Lane 1: Unbroken *E. coli* C41 cells; Lane 2: Broken *E. coli* C41 cells; Lane 3: Soluble fraction; Lane 4: Fraction washed with 2 M of NaCl; Lane 5: Membrane fraction; Lane 6: Membranes; M- PeqGold protein marker. Red box shows the band with the size of MQO 1 from *S. aureus*. .... 22

**Figure 4.4-** Chromatogram obtained from the purification of MQO 1 from *S. aureus* using an Histrap HP (5 mL) column. Buffer A: 50 mM potassium phosphate pH 7, 10 % glycerol, 250 mM NaCl; Buffer B: 50 mM potassium phosphate pH 7, 10 % glycerol, 250 mM NaCl, 250 mM Histidines. The dark grey line represents the Abs<sub>280nm</sub> and in light grey line the % of 250 mM Histidines is represented. Red box corresponds to the MQO 1 from *S. aureus* peak fraction..... 22

**Figure 4.5-** SDS-PAGE gel and UV-Visible spectrum of the isolated MQO 1 from *S. aureus*. **A-** SDS-PAGE gel of the purified MQO 1 *S. aureus* (molecular mass: ~ 57 kDa) . SDS-PAGE gel: Stacking and Resolving gel – 15 % acrylamide. M- PeqGold protein marker was used; Red box shows the band corresponding to MQO 1 from *S. aureus*. **B-** UV-Visible spectrum of the isolated MQO 1 from *S. aureus* in 50 mM potassium phosphate pH 7, 10 % glycerol, 250 mM NaCl (diluted 1:10). The insert highlights the region between 250 and 550 nm. .... 23

**Figure 4.6-** SDS-PAGE gel with the samples from all the steps in MQO 2 from *S. aureus* purification process. SDS-PAGE gel: Stacking and Resolving Gel – 15 % acrylamide. Molecular mass of MQO 2 (*S. aureus*): ~ 55 kDa; Lane 1: Unbroken *E. coli* C41 cells; Lane 2: Broken *E. coli* C41 cells; Lane 3: Soluble fraction; Lane 4: Fraction washed with 2 M of NaCl; Lane 5: Membrane fraction; Lane 6: Membranes; M- PeqGold protein marker. Red box shows the band with the size of MQO 2 from *S. aureus*. .... 24

**Figure 4.7-** Chromatograms obtained from the purification of MQO 2 from *S. aureus* using an Histrap HP (5 mL). **A-** Chromatogram obtained with the injection of soluble fraction of MQO 2 from *S. aureus*; **B-** Chromatogram obtained by the injection of membrane fraction of MQO 2 from *S. aureus*; Buffer A: 50 mM potassium phosphate pH 7, 10 % glycerol, 250 mM NaCl; Buffer B: 50 mM potassium phosphate pH 7, 10 % glycerol, 250 mM NaCl, 250 mM Histidines. The dark grey line represents the Abs<sub>280nm</sub>, in light grey line the % of 250 mM Histidines is represented. Red boxes correspond to MQO 2 from *S. aureus* elution. .... 24

**Figure 4.8-** Chromatograms obtained from the purification of MQO 2 from *S. aureus* using a Q-Sepharose HP (64 mL) column. **A-** Chromatogram obtained with the injection of soluble fraction of MQO 2 from *S. aureus*; **B-** Chromatogram obtained by the injection of membrane fraction of MQO 2 from *S. aureus*; Buffer A: 100 mM potassium phosphate pH 7; Buffer B: 100 mM potassium phosphate pH 7, 1 M NaCl. The dark grey line represents the Abs<sub>280nm</sub>, in light grey line the % of 1 M NaCl is represented. Red boxes correspond to MQO 2 from *S. aureus* elution. .... 25

**Figure 4.9-** UV-Visible spectra and SDS-PAGE gel of the isolated MQO 2 from *S. aureus*. **A-** UV-Visible spectrum of Fraction A; **B-** UV-Visible spectrum of Fraction B; Samples in 50 mM potassium phosphate pH 7, 10 % glycerol, 250 mM NaCl. The figures show a zoom of the region between 250 and 550 nm; **C-** SDS-PAGE gel of the purified MQO 2 *S. aureus* (molecular mass: ~ 55 kDa); SDS-PAGE gel: Stacking and Resolving Gel – 15 % acrylamide; Lane 1- Fraction B; Lane 2- Fraction A; M- PeqGold protein marker. Red box shows the band corresponding to MQO 2 from *S. aureus*. .... 26

**Figure 4.10-** SDS-PAGE gel of the samples from all the steps of MQO from *E. coli* along the purification process. SDS-PAGE gel: Stacking and Resolving Gel – 15 % acrylamide. Molecular mass of MQO (*E. coli*): ~ 60 kDa; Lane 1: Broken *E. coli* Rosetta cells; Lane 2: Soluble fraction; Lane 3: Fraction washed with 2 M of NaCl; Lane 4: Membrane fraction; Lane 5: Membranes; M- PeqGold protein marker. Red box shows the band with the size of MQO from *E. coli*. .... 27



**Figure 4.11-** Chromatogram obtained from the purification of MQO from *E. coli* using an Histrap HP (5 mL) column. **A-** Chromatogram obtained with the injection of soluble fraction of MQO from *E. coli*; **B-** Chromatogram obtained by the injection of membrane fraction of MQO from *E. coli*; Buffer A: 50 mM potassium phosphate buffer pH 7, 10 % glycerol, 250 mM NaCl; Buffer B: 50 mM potassium phosphate pH 7, 10 % glycerol, 250 mM NaCl, 250 mM Histidines. The dark grey line represents the Abs<sub>280nm</sub>, in light grey line the % of 250 mM Histidines is represented. Red boxes correspond to MQO from *E. coli* elution. .... 27

**Figure 4.12-** Chromatogram obtained from the purification of membrane fraction of MQO from *E. coli* using a Q- Sepharose HP (64 mL) column. Buffer A: 100 mM potassium phosphate pH 7; Buffer B: 100 mM potassium phosphate pH 7, 1 M NaCl, pH 7. The dark grey line represents the Abs<sub>280nm</sub>, in light grey line the % of 1 M NaCl is represented. Red box corresponds to MQO from *E. coli* elution. .... 28

**Figure 4.13-** UV-Visible spectra and SDS-PAGE gel of the purified MQO from *E. coli*. **A-** UV-Visible spectrum of Fraction A (diluted 1:10); **B-** UV-Visible spectrum of Fraction B; Samples in 50 mM potassium phosphate pH 7, 10 % glycerol, 250 mM NaCl. The figures show a zoom in the region between 250 and 550 nm; **C-** SDS-PAGE gel of Fraction A (MQO from *E. coli*); **D-** SDS-PAGE gel of Fraction B (MQO from *E. coli*); Molecular mass of MQO (*E. coli*): ~ 60 kDa; SDS-PAGE gel: Stacking and Resolving Gel – 15 % acrylamide. M- PegGold protein marker. Red boxes show the band corresponding to MQO from *E. coli*. .... 29

**Figure 4.14-** Blue Native PAGE gel with MQO 1 from *S. aureus* (molecular mass: ~ 57 kDa); Acrylamide gel- 4 a 16 %; M- Marker for Native PAGE. Red box shows the band corresponding to MQO 1 from *S. aureus*. .... 31

**Figure 4.15-** Catalytic activity assays with MQO 1 from *S. aureus* (**A**), MQO 2 from *S. aureus* (**B** and **C**) and MQO from *E. coli* (**D**). Assays done in aerobic conditions, using scavenging system, at 37 °C in 50 mM potassium phosphate pH 7, 10 % glycerol, 250 mM NaCl. .... 32

**Figure 4.16-** pH profile of MQO 1 from *S. aureus* (**A**) and of MQO from *E. coli* (**B**). Assays were performed under anaerobic conditions, using scavenging system, at 37 °C, in 50 mM potassium phosphate, 10 % glycerol, 250 mM NaCl pH values between 6 and 8. Each point, presented with error bars, corresponds to duplicate experiments using 100 µM DMN, 3000 µM malate and 125 nM of MQO 1 from *S. aureus* or 250 nM of MQO from *E. coli*. .... 34

**Figure 4.17-** UV-Visible spectrum of MQO 1 from *S. aureus* oxidized (light grey) and reduced (dark grey) with 1000 µM malate, in 50 mM potassium phosphate pH 7, 10 % glycerol, 250 mM NaCl. Spectra were obtained under anaerobic conditions ensured by the scavenging system, 37 °C using 10 µM MQO1 from *S. aureus*. The inserted figure expands absorption spectrum in the 250–550 nm region. .... 34

**Figure 4.18-** Steady-state analyses of MQO 1 from *S. aureus* and of MQO from *E. coli*. Malate:quinone oxidoreductase activity as function of the concentration of DMN (**A**) or malate (**B**) using 125 nM MQO 1 from *S. aureus*. Malate:quinone oxidoreductase activity as function of the concentration of DMN or DDB (**C**) or malate (**D**) using 250 nM MQO from *E. coli*. The data points were fitted with a Michaelis-Menten equation (full line),  $V_0 = (V_{max} [S]) / (K_M + [S])$ . All the assays were done under anaerobic conditions, using a scavenging system, at 37 °C in 50 mM potassium phosphate pH 7, 10 % glycerol, 250 mM NaCl... .... 36

**Figure 4.19-** Steady-state analyses of the activity of MQO 1 from *S. aureus* in the presence of HQNO. Inhibition assays were performed in the presence of 3000 µM malate, 100 µM DMN, 125 nM MQO 1 from *S. aureus*, under anaerobic conditions, using scavenging system, at 37 °C in 50 mM potassium phosphate pH 7, 10 % glycerol, 250 mM NaCl. The concentrations of HQNO tested were 0,1, 5, 10, 50 and 100 µM. .... 37

**Figure 4.20-** Steady-state analyses of the activity of MQO 1 from *S. aureus* in the presence of two different concentrations of HQNO. Malate:quinone oxidoreductase activity as function of the concentration of DMN (**A**) or malate (**B**) using 125 nM MQO 1 from *S. aureus* in the presence of 0  $\mu$ M (circles), 10  $\mu$ M (squares) or 20  $\mu$ M (triangles) of HQNO; All assays were performed under anaerobic conditions, using scavenging system, at 37 °C in 50 mM potassium phosphate pH 7, 10 % glycerol, 250 mM NaCl..... 38

**Figure 4.21-** Protein-substrate interaction studies. **A-** Change in fluorescence emission at 330 nm with excitation at 295 nm of MQO 1 from *S. aureus* by sequential addition of DMN (closed circles) and in the presence of HQNO (open circles); **B-** Change in the fluorescence emission at 330 nm with excitation at 280 nm of MQO 1 from *S. aureus* by sequential addition of oxaloacetate (closed triangles) and in the presence of HQNO (open triangles). **C-** Change in the fluorescence emission at 330 nm with excitation at 280 nm of MQO 1 from *S. aureus* by sequential addition of HQNO (open squares). The solid lines were obtained by fitting the data using the equation  $\Delta F = \Delta F_{max} \times [S] / (K_D + [S])$ ..... 40

**Figure 7.1-** Flavin adenine nucleotide UV-Visible spectrum..... 49

**Figure 7.2-** UV-Visible spectra of oxidized (light grey) and reduced (dark grey) DMN (A) or DDB (B) with NaBH<sub>4</sub>. A- The  $\Delta$ Abs is higher at 270 nm. B- The  $\Delta$ Abs is higher at 278 nm.  $\Delta$ Abs represents the difference in the absorbance between oxidized and reduced spectra. Spectra obtained in an anaerobic chamber, using 20  $\mu$ M or 75  $\mu$ M of DMN or DDB, respectively, and 2 mM of NaBH<sub>4</sub>. ..... 49

**Figure 7.3-** Mass Spectrometry Unit Assay Report. Report of the analysis to the identification of the protein purified. .... 51

**Figure 7.4-** Reactions of Scavenging System. (1)- Glucose Oxidase consumes oxygen and glucose to form hydrogen peroxide. (2)- Catalase consumes the hydrogen peroxide formed in (1) and yielding molecular oxygen and water. .... 51

## **Index of tables**

<b>Table 3.1-</b> Conditions tested for the expression of the different MQO, using <i>E. coli</i> Rosetta cells. Expression tests of the genes coding for MQO 1 from <i>Staphylococcus aureus</i> (MQO 1 <i>S. aureus</i> ), MQO 2 from <i>Staphylococcus aureus</i> (MQO 2 <i>S. aureus</i> ), MQO from <i>Escherichia coli</i> (MQO <i>E. coli</i> ), MQO from <i>Helicobacter pylori</i> (MQO <i>H. pylori</i> ), MQO from <i>Plasmodium falciparum</i> (MQO <i>P. falciparum</i> )....	11
<b>Table 3.2-</b> Conditions tested for the expression of the different MQOs using <i>E. coli</i> C43 pLysS cells. Expression tests of the genes coding for MQO 1 from <i>Staphylococcus aureus</i> (MQO 1 <i>S. aureus</i> ), MQO 2 from <i>Staphylococcus aureus</i> (MQO 2 <i>S. aureus</i> ), MQO from <i>Escherichia coli</i> (MQO <i>E. coli</i> ), MQO from <i>Helicobacter pylori</i> (MQO <i>H. pylori</i> ), MQO from <i>Plasmodium falciparum</i> (MQO <i>P. falciparum</i> )..	11
<b>Table 3.3-</b> Conditions tested for the expression of the different MQOs using <i>E. coli</i> C41 cells. Expression tests of the genes coding for MQO 1 from <i>Staphylococcus aureus</i> (MQO 1 <i>S. aureus</i> ), MQO 2 from <i>Staphylococcus aureus</i> (MQO 2 <i>S. aureus</i> ), MQO from <i>Helicobacter pylori</i> (MQO <i>H. pylori</i> ) and MQO from <i>Plasmodium falciparum</i> (MQO <i>P. falciparum</i> ).....	12
<b>Table 4.1-</b> Results of the expression tests for the genes coding for the different MQOs. The table shows the conditions tested in the expression tests and respective results. (✓) - Represent the results in which a band with the expected size for each protein was observed in a SDS-PAGE gel. ....	19
<b>Table 4.2-</b> Quantification of total protein and flavin content of the samples of MQO 1 and MQO 2 from <i>S. aureus</i> and MQO from <i>E. coli</i> . ....	30
<b>Table 4.3-</b> Retention times of the flavin prosthetic groups. Retention times of the standards (FAD and FMN) and sample injected in a reverse phase column operated in a HPLC system.....	31
<b>Table 4.4-</b> Kinetic parameters of MQO 1 from <i>S. aureus</i> obtained for DMN in the presence of 0, 10 and 20 $\mu$ M HQNO. Determination of kinetic parameters was done using the Michaelis-Menten equation...	38
<b>Table 4.5-</b> Kinetic parameters of MQO 1 from <i>S. aureus</i> obtained for malate in the presence of 0, 10 and 20 $\mu$ M HQNO. Determination of kinetic parameters was done using the Michaelis-Menten equation....	39
<b>Table 4.6-</b> Substrate-enzyme dissociation constants of MQO 1 from <i>S. aureus</i> determined for both substrates in the absence and in the presence of HQNO. ....	41
<b>Table 7.1-</b> Compositions of the media used to perform expression tests and cell growth. ....	49
<b>Table 7.2-</b> Composition of the solutions used in SDS-PAGE and NATIVE PAGE gels. ....	50
<b>Table 7.3-</b> Kinetic parameters of MQO 1 from <i>S. aureus</i> obtained for DMN and malate. Determination of kinetic parameters was done using the Michaelis-Menten equation. ....	52
<b>Table 7.4-</b> Kinetic parameters of MQO from <i>E. coli</i> obtained for DDB and DMN. Determination of kinetic parameters was done using the Michaelis-Menten equation. ....	52
<b>Table 7.5-</b> Kinetic parameters of MQO from <i>E. coli</i> obtained for malate using DDB and DMN. Determination of kinetic parameters was done using the Michaelis-Menten equation. ....	52



## **List of abbreviations**

2YT: Yeast Extract and Tryptone

Abs: absorbance

Acetyl-CoA: acetyl coenzyme A

APS: ammonium persulfate

ATP: adenosine triphosphate

BCA: Bicinchoninic Acid Protein Assay

BSA: bovine serum albumin

Cp I: complex I

Cp II: complex II

Cp III: complex III

Cp IV: complex IV

DDB: 2,3-Dimethoxy-5,6-dimethyl-p-benzoquinone

DMN: 2,3-Dimethyl-1,4-naphthoquinone

*E. coli*: *Escherichia coli*

*P. falciparum*: *Plasmodium falciparum*

FAD: flavin adenine dinucleotide

FMN: flavin mononucleotide

G3P: glycerol-3-Phosphate

*H. pylori*: *Helicobacter pylori*

HPLC: high performance liquid chromatography

HQNO: 2-n-Hepthyl-4-hydroxyquinoline-N-oxide

IPTG: isopropyl- $\beta$ -D-thiogalactosidase

LB: Luria Bertani

LQO: lactate:quinone oxidoreductase

MDH: malate dehydrogenase, malate:NAD<sup>+</sup> oxidoreductase

MQO: malate:quinone oxidoreductase

MS: mass spectrometry

NAD<sup>+</sup>: oxidized nicotinamide adenine dinucleotide

NADH: reduced nicotinamide adenine dinucleotide

OD<sub>600</sub>: optical density at 600 nm

Q: quinone

QH<sub>2</sub>: quinol

Rpm: rotations per minute

*S. aureus*: *Staphylococcus aureus*

SDS: sodium dodecyl sulphate

SDS-PAGE: sodium dodecyl sulphate – polyacrylamide gel electrophoresis

TB: terrific Broth

TCA: tricarboxylic acid

TEMED: tetramethylethylenediamine

# **1. Introduction**

## **1.1. Energetic metabolism**

Energy is involved in most biochemical reactions needed for the cell life. Cellular metabolism, the set of all reactions taking place in an organism, can be divided in two groups of reactions, catabolism and anabolism. Catabolism includes mainly favorable thermodynamic reactions that degrade complex macromolecules into simpler molecules, releasing energy. In the case of anabolism, most reactions need energy input for the synthesis of biomolecules, important for the living cell, from simpler precursors<sup>1</sup>.

The free energy released by catabolic reactions powers the anabolic ones, and for that this energy must be converted to other forms. Besides ATP synthesis, the free energy released from catabolic reactions may be converted and conserved in the form of a transmembrane difference in electrochemical potential established by the translocation of ions across the cellular or mitochondrial membranes. The establishment of the electrochemical potential is possible due to the action of proteins of the respiratory chain that couple the oxidoreduction reactions to the translocation of protons against their electrochemical potential, and due to the impermeability of the membranes to ions. This electrochemical potential may in turn power several needs of the cell, such as ATP synthesis, solute transport or motility<sup>1,2</sup>.

The central catabolic pathway of carbohydrates is glycolysis, in which glucose, an energy source for animals, plants and other organisms, is converted into pyruvate. This metabolic process is a series of reactions catalyzed by several enzymes that release some free energy which is stored in the form of ATP and NADH<sup>2,3,4</sup>.

The pyruvate formed in the glycolysis can be used in different catabolic reactions, such as the Tricarboxylic Acid Cycle (TCA). This cycle represents a central pathway in the cell metabolism and is a converging point of the catabolic pathways of carbohydrates, fatty acids and amino acids. The cycle allows the flux in the catabolic pathways of the different macromolecules, and it provides substrates to the respiratory chain. In this way, it allows indirect energy conservation by ATP synthesis and establishment of the membrane potential<sup>2,4</sup>.

## **1.2. The role of malate:quinone oxidoreductases in metabolism**

Malate:quinone oxidoreductases (MQOs) are responsible for the oxidation of malate to oxaloacetate and the reduction of quinone to quinol. This enzyme is present in some microorganisms but absent in humans. Usually organisms with mitochondria have the soluble malate:NAD<sup>+</sup> oxidoreductase or a malate dehydrogenase (MDH). This enzyme also oxidizes L-malate to oxaloacetate but instead of reducing the quinone, this protein reduces NAD<sup>+</sup> to NADH. Both MQO and MDH are involved in the TCA cycle. Some organisms present genes coding for the two proteins. In this case it is yet not clear in which situation each of the enzymes is expressed. The catalyzed reactions are thermodynamically very different; the  $\Delta G^{\circ}$  involved in the reaction of MQO is -55 or -18.9 kJ.mol<sup>-1</sup>, for ubiquinone or

menaquinone, respectively, whereas  $\Delta G^{\circ'}$  involved in the reaction of MDH is  $+28.6 \text{ kJ.mol}^{-1}$ , which makes it thermodynamically unfavorable. MDH reaction seems to take place due to the high rate of oxaloacetate's removal by citrate synthase<sup>5,6,7,8,9</sup>.

### 1.2.1. Tricarboxylic Acid Cycle as a central metabolic pathway

The Tricarboxylic Acid (TCA) cycle, also called citric acid cycle or Krebs cycle, is the major final common pathway of oxidation of carbohydrates, lipids and proteins, since the oxidation of these molecules yields acetyl-CoA or several intermediate metabolites of the cycle. The intermediates of this cycle can also be important to the biosynthetic pathway of fatty acids, proteins and carbohydrates, as shown in Figure 1.1. In this way, the TCA cycle presents a central role in both catabolic and anabolic metabolisms<sup>2,4,10</sup>.

TCA, schematically represented in Figure 1.1, takes place in the mitochondrial matrix in eukaryotes and in the cytosol in prokaryotic organisms. This metabolic pathway is constituted by chain reactions catalyzed by eight enzymes, starting by the condensation of oxaloacetate using acetyl-CoA and ending with the formation of oxaloacetate from malate, before the beginning of a new cycle. In the end, for each molecule of acetyl-CoA used, three NADH molecules, one ATP and one quinol molecule are formed. These molecules can be used in other pathways as the respiratory chain, reinforcing the central role of this cycle<sup>4,11</sup>.

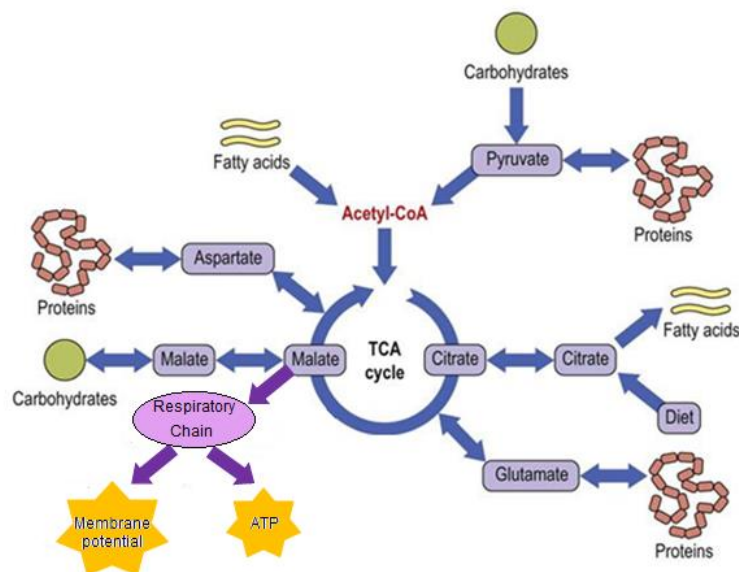


**Figure 1.1-** Schematic representation of metabolic pathways. Metabolic pathways converging in the Tricarboxylic Acid Cycle. Adapted from<sup>10</sup>.

The last step of the TCA cycle is the oxidation of malate to oxaloacetate and this reaction can be catalyzed by two different enzymes, MQO and MDH, as described above. In addition, MQO reduces the quinone to quinol, in this way being also directly involved in the respiratory chain<sup>6,8</sup>.



### 1.2.2. Respiratory chain

Respiratory chains are very diverse and evolved according to the specific metabolic needs of each organism. However, in all organisms, the respiratory chain is composed of several proteins and protein complexes with oxidoreduction activity. Some of these membrane proteins can use the free energy released by the catalytic reactions to perform the thermodynamically unfavorable ion translocation, protons or charges, contributing in this way for the establishment of the membrane potential.

The canonical/mitochondrial respiratory chain, the most studied electron transport chain, is composed of four different complexes, I to IV. These complexes are responsible for the electron transfer from the electron donors, NADH and succinate, to the final electron acceptor,  $O_2$ . The representation of complexes of the mammalian respiratory chain is shown in Figure 1.2<sup>12</sup>.

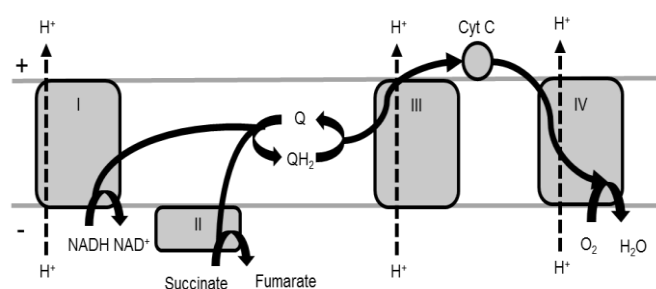


**Figure 1.2-** Representation of the canonical/mitochondrial respiratory chain. Four complexes are present in this respiratory chain and the arrangement of the complexes as proposed to date is represented. (+) and (-) indicate the positive and negative sides of the transmembrane difference in the electrochemical potential, respectively.

Complex I (Cp I) is the largest complex of the respiratory chain complexes, formed by ~44 polypeptides. It is an “L” shaped complex and has as cofactors one flavin (FMN) and 8 iron-sulfur centers. Cp I is responsible for the transfer of 2 electrons from NADH to the quinone and couples the free energy released by this oxidoreduction reaction to the translocation of protons across the membrane<sup>13, 14</sup>.

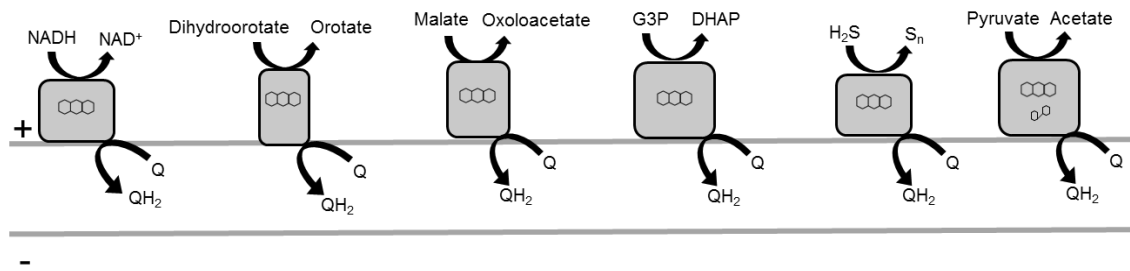
Complex II (Cp II) catalyzes the oxidation of succinate to fumarate with reduction of quinone (Q) to quinol ( $QH_2$ ). This is the only mitochondrial respiratory complex that does not translocate charges across the membrane<sup>15</sup>.

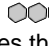
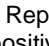
Complex III (Cp III) catalyzes the electron transfer from the quinol to cytochrome *c*. This reaction is coupled to the translocation of charges across the membrane. This complex is a transmembrane complex protein composed of three catalytic subunits (cytochrome  $c_1$ , cytochrome *b* and Rieske iron-sulfur subunit).

Cytochrome *c* is responsible for reducing complex IV (Cp IV), also called cytochrome *c* oxidase, which has thirteen subunits, but only two of them are directly involved in the catalytic activity. This is the final step of the electron transfer chain. In this step cytochrome *c* is oxidized and  $O_2$  is reduced to two water molecules (cytochrome *c*: $O_2$  oxidoreductase), translocating protons across the membrane<sup>12</sup>.

The mammalian respiratory chain seems to be quite simple when comparing to the diversity of the respiratory chains from other organisms. The respiratory chains from other organisms can also include other proteins and protein complexes performing different reactions, and have additional electron acceptors instead of oxygen. These diversity and flexibility are also reflected by the different substrates,

such as lactate, pyruvate, dihydroorotate, malate, among others. These substrates can be used by several quinone reductases, X:quinone oxidoreductases (Figure 1.3)<sup>16</sup>.



**Figure 1.3-** Schematic representation of X:quinone oxidoreductases present in the respiratory chain of *Staphylococcus aureus*.  - Representation of the flavin.  - Representation of the thiamine diphosphate (TPP). (+) and (-) indicates the positive and negative sides of the transmembrane difference in the electrochemical potential, respectively. Adapted from<sup>16</sup>.

MQO is an example of a monotopic protein, it is attached to the membrane from one side, and oxidizes malate and reduces the quinone. These proteins are considered electron entry points of the respiratory chain, since these enzymes can oxidize different substrates and feed the quinone pool of the respiratory chain<sup>17</sup>.

### 1.2.3. Other metabolic pathways

The ability to survive in different environments is the reason for the diversity of the energetic metabolisms in microorganisms. Some organisms use different pathways to satisfy their energetic needs. In addition to the TCA cycle and the respiratory chain, there are other metabolic pathways such as the fumarate cycle, shown in Figure 1.4<sup>5,18</sup>.

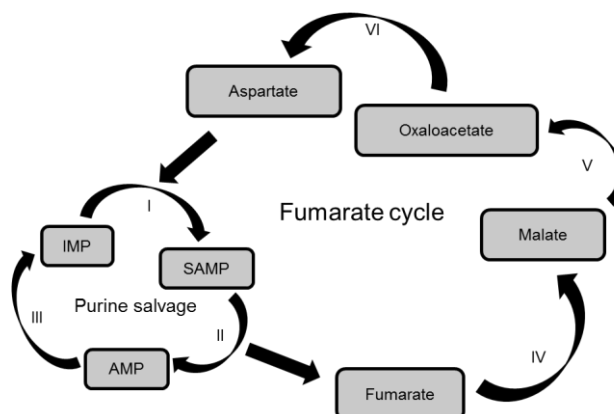


**Figure 1.4-** Representation of the Fumarate cycle in *Plasmodium falciparum*. Enzymes involved in the Fumarate cycle: I- Adenylosuccinate synthetase; II- Adenylosuccinate lyase; III- Adenosine monophosphate deaminase; IV- Fumarate hydratase; V- Malate:quinone oxidoreductase; VI- Aspartate aminotransferase. Substrates of the Purine salvage pathway: IMP- Inosine monophosphate; SAMP- Adenylosuccinate; AMP- Adenosine monophosphate<sup>18</sup>.

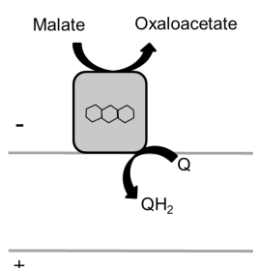
The fumarate cycle starts with the conversion of fumarate to malate that is oxidized by MQO to oxaloacetate. Then, oxaloacetate is transported to the cytoplasm, here being the substrate of the reaction catalyzed by aspartate aminotransferase to form aspartate. Aspartate enters the purine

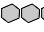
salvage, a way to recycle purine bases instead of synthesizing them *de novo*, in which fumarate is released. MQO is important in this cycle to provide the oxaloacetate needed in the cytosol to be converted to aspartate<sup>5</sup>.

### 1.3. Malate:quinone oxidoreductases

From all the enzymes described above, MQO is a protein with a remarkable role in the energetic metabolism of the organisms, as part of TCA cycle, respiratory chains or other pathways, like the fumarate cycle. Surprisingly, this protein has not been fully characterized to date, and no structural data are available yet. There are some studies describing the biochemical characterization of MQO, but none of them accomplished to isolate the protein.

Malate:quinone oxidoreductase (EC 1.1.5.4) is a monotopic protein that is linked to the surface of the membrane by electrostatic and hydrophobic interactions. This protein was first described in *Micrococcus lysodeikticus* in 1950 and since then it has been studied in several other organisms, such as *Bacillus sp. PS3*, *Corynebacterium glutamicum*, *Helicobacter pylori* and *Escherichia coli*<sup>6,7,8,9,19</sup>.



**Figure 1.5-** Representation of malate:quinone oxidoreductases. - Representation of the flavin. (+) and (-) indicates the positive and negative sides of the transmembrane difference in the electrochemical potential, respectively. Adapted from<sup>16</sup>.

MQO has a flavin adenine dinucleotide (FAD) as a prosthetic group, shown in Figure 1.5 as well as the catalytic activity of MQO. This prosthetic group has an extinction coefficient of  $11.3 \text{ mM}^{-1}\text{cm}^{-1}$  and has a characteristic UV-Visible spectrum (Figure 7.1, in appendix), which has bands with maxima at 375 and 450 nm. This maximum of absorption at 450 nm is responsible for the yellow color of the protein<sup>20</sup>. In the sequence of MQO there is a conserved hydrophobic motif in the N-terminal region. This motif is also found in the N-terminal of the glycerol-3-phosphate dehydrogenases and is known as a part of the FAD-binding site<sup>7,8</sup>.

#### 1.3.1. MQOs in pathogenic organisms

MQOs are present in different organisms and according to a study where a taxonomic profile was performed for several protein complexes including MQOs, this enzyme is described to be present in the three domains of life, in Bacteria (27 %), Archaea (9 %) and Eukarya (5 %)<sup>16</sup>.

For this study, we selected the MQOs from *Staphylococcus aureus*, *Escherichia coli*, *Helicobacter pylori* and *Plasmodium falciparum*. The selection of these organisms was based at first on their pathogenicity

and threat for human health. Since MQO is absent in humans, this protein may be considered a potential drug target to produce pharmaceuticals against these pathogens. In addition, these organisms synthesize different quinones, ubiquinones and menaquinones and thus this study will allow us to explore possible structural and functional specificities towards the different substrates<sup>9,21</sup>.

#### 1.3.1.1. *Staphylococcus aureus*

*Staphylococcus aureus* belongs to the Micrococcaceae family, being a spherical coccus, non-sporing and Gram-positive bacterium. These microorganisms are facultative anaerobes, depending on the surrounding environment, and can be found in the human respiratory tract and in the skin<sup>22,23</sup>.

*S. aureus* is one of the causes of respiratory diseases and is one of the five most common causes of hospital-acquired infections. The treatment for *S. aureus* infection involves penicillin, but from year to year the number of penicillin-resistant isolates has been growing and the treatment of *S. aureus* infection has become a challenge<sup>24,25,26</sup>.

*S. aureus* has two genes that code for MQO, one for MQO 1 and the other one for MQO 2<sup>27</sup>.

#### 1.3.1.2. *Escherichia coli*

*Escherichia coli* is a Gram-negative, non-sporing and non-capsulated bacterium. It is a microorganism that is usually found in human or animal intestine.

These bacteria are responsible for many of the humans' infections, from urinary tract infection to septicemia. Although it is a well-studied organism and widely used as a biologic model, it is still one of the leading causes of hospital infections<sup>23,28</sup>.

This microorganism has both enzymes to catalyze the oxidation of malate to oxaloacetate, MQO and MDH. It is not clear in which situation each enzyme is expressed, but according to the Gibbs standard free energy, the reaction using MQO is more favorable. In *E. coli*, the quinone used by MQO is dependent on the growth conditions, in aerobiosis it expresses ubiquinone and in anaerobic conditions, menaquinone is the preferred quinone<sup>6,8,21</sup>.

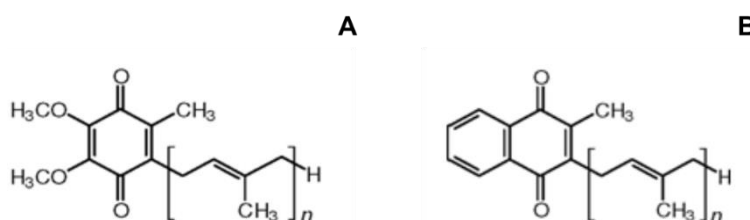


**Figure 1.6-** Quinones chemical structure. A- Structure of Ubiquinone analog (DDB); B- Structure of Menaquinone analog (DMN).

#### 1.3.1.3. *Helicobacter pylori*

*Helicobacter pylori* is a Gram-negative spirally shaped bacterium that colonizes the stomach and small intestine. This microorganism is a strict microaerophile and has strong urease activity.

These bacteria are one of the most common causes of human infections since this microorganism may be transmitted via water. *H. pylori* is commonly associated with diseases such as gastritis, peptic and gastric ulcers and gastric cancer<sup>23,29</sup>.

Biochemical measurements done with *H. pylori* indicated that MDH activity was present but looking at the genome, there is no gene coding for a MDH enzyme. This led to the hypothesis that *H. pylori* has a gene coding for MQO, and MQO was first described in this microorganism in 2000<sup>7</sup>.

#### 1.3.1.4. *Plasmodium falciparum*

*Plasmodium falciparum* is an intracellular parasite that normally grows and replicates within a non-phagosomal vacuole. The life cycle of this parasite is very complex, requiring specific proteins in each stage of the cycle, meaning that all proteins are important for parasite survival<sup>30</sup>.

*P. falciparum* is the cause of the most severe malaria in humans. Due to the absence of treatments and the emerging drug resistance of the parasites, the development of novel treatments and vaccines are very demanding<sup>5,11</sup>.

In this microorganism, MQO is involved in the TCA cycle, the respiratory chain and the fumarate cycle and is described as essential for parasite survival at specific stages of its sexual cycle. Thus, this protein from these microorganisms is an important target to study<sup>5,18</sup>.



## **2. Objectives**

Malate:quinone oxidoreductases (MQOs) are membrane bound enzymes that oxidize malate to oxaloacetate and reduce quinone to quinol. These enzymes can be found in different organisms, such as *Escherichia coli*, *Staphylococcus aureus*, *Helicobacter pylori* and *Plasmodium falciparum*. MQOs are absent in mammalian mitochondria, making them potential drug targets.

The goal of this dissertation is the biochemical and functional characterization of MQOs in order to understand their importance within the organisms.

The specific objectives are:

- Optimize the expression and the purification of MQOs;
- Characterize biochemically and functionally these proteins;
- Study the interaction between the proteins and the respective substrates.





### 3. Materials and Methods

At the beginning of this project five plasmids, each one with the gene coding for one MQO, MQO 1 from *Staphylococcus aureus* (NCBI protein ID: CCJ21484), MQO 2 from *Staphylococcus aureus* (NCBI protein ID: CCJ21678), MQO from *Escherichia coli* (NCBI protein ID: 16130147), MQO from *Helicobacter pylori* (NCBI protein ID: XP\_966154) and MQO from *Plasmodium falciparum* (NCBI protein ID: NP\_206886), were already available in the host lab. These five plasmids were used in expression tests, in which different conditions were assessed, including different cell types, media, growth extension and presence or absence of the inducer.

#### 3.1. Expression Tests

The selected cells (*E. coli* Rosetta, *E. coli* C43 pLysS and *E. coli* C41) used in each expression test and later in large scale cell growth were transformed with the plasmid pET-28a(+) containing the coding gene for each MQO of interest. The transformation was performed using a heat shock method<sup>31</sup>.

Expression tests were made in order to find the best conditions to express the gene coding for each of the five selected malate:quinone oxidoreductases (MQOs). The conditions tested in these 50 mL tests are summarized in the Tables 3.1, 3.2 and 3.3.

**Table 3.1-** Conditions tested for the expression of the different MQO, using *E. coli* Rosetta cells. Expression tests of the genes coding for MQO 1 from *Staphylococcus aureus* (MQO 1 *S. aureus*), MQO 2 from *Staphylococcus aureus* (MQO 2 *S. aureus*), MQO from *Escherichia coli* (MQO *E. coli*), MQO from *Helicobacter pylori* (MQO *H. pylori*), MQO from *Plasmodium falciparum* (MQO *P. falciparum*).

Protein	MQO 1 <i>S. aureus</i> , MQO 2 <i>S. aureus</i> , MQO <i>E. coli</i> , MQO <i>H. pylori</i> , MQO <i>P. falciparum</i>							
Cell type	<i>E. coli</i> Rosetta							
Medium	Yeast Extract and Tryptone (2YT)		Luria Bertani (LB)		Terrific Broth (TB)			
Growth time	4 hours	Overnight	4 hours	Overnight	4 hours	Overnight		
Inducer	+	+	+	+	+	-	+	-

Note: Protein expression induced with IPTG (+) and protein expression without induction (-).

**Table 3.2-** Conditions tested for the expression of the different MQOs using *E. coli* C43 pLysS cells. Expression tests of the genes coding for MQO 1 from *Staphylococcus aureus* (MQO 1 *S. aureus*), MQO 2 from *Staphylococcus aureus* (MQO 2 *S. aureus*), MQO from *Escherichia coli* (MQO *E. coli*), MQO from *Helicobacter pylori* (MQO *H. pylori*), MQO from *Plasmodium falciparum* (MQO *P. falciparum*).

Protein	MQO 1 <i>S. aureus</i> , MQO 2 <i>S. aureus</i> , MQO <i>E. coli</i> , MQO <i>H. pylori</i> , MQO <i>P. falciparum</i>					
Cell type	<i>E. coli</i> C43 pLysS					
Medium	Yeast Extract and Tryptone (2YT)		Luria Bertani (LB)		Terrific Broth (TB)	
Growth time	4 hours		4 hours		4 hours	Overnight
Inducer	+		+		+	-

Note: Protein expression induced with IPTG (+) and protein expression without induction (-).

**Table 3.3-** Conditions tested for the expression of the different MQOs using *E. coli* C41 cells. Expression tests of the genes coding for MQO 1 from *Staphylococcus aureus* (MQO 1 *S. aureus*), MQO 2 from *Staphylococcus aureus* (MQO 2 *S. aureus*), MQO from *Helicobacter pylori* (MQO *H. pylori*) and MQO from *Plasmodium falciparum* (MQO *P. falciparum*).

Protein	MQO 1 <i>S. aureus</i> , MQO 2 <i>S. aureus</i> , MQO <i>H. pylori</i> , MQO <i>P. falciparum</i>					
Cell type	<i>E. coli</i> C41					
Medium	Yeast Extract and Tryptone (2YT)		Luria Bertani (LB)		Terrific Broth (TB)	
Growth time	4 hours		4 hours		4 hours	Overnight
Inducer	+		+		+	-

Note: Protein expression induced with IPTG (+) and protein expression without induction (-).

In all tests the expression was induced with 1 mM of IPTG (isopropyl- $\beta$ -D-thiogalactosidase) (Apollo Sientific), at an optical density of 0.6 (OD<sub>600</sub>). Samples before and after induction were collected. The expression of each protein was evaluated by SDS-PAGE (sodium dodecyl sulphate – polyacrylamide gel electrophoresis). Samples were normalized by OD<sub>600</sub> and collected by centrifugation for 5 minutes, at 2404 xg. The *pellet* was resuspended in 5  $\mu$ L of loading buffer and 5  $\mu$ L of water. Samples were boiled for 5 minutes, injected in a 15 % acrylamide gel and subjected to 180 V for 1:30 hour, using a Mini-PROTEAN® Electrophoresis System (BIORAD). PeqGold protein marker was used in the case of MQO 1 from *S. aureus*, MQO 2 from *S. aureus* and MQO from *H. pylori* samples and for the samples corresponding to MQO from *E. coli*, Low molecular weight protein marker was used. Coomassie brilliant blue was used to stain the gel after excess removal by a destaining solution was used.

## 3.2. Cell growth

The most promising results in expression tests were those corresponding to the expression of the gene coding for MQOs from *Staphylococcus aureus* and *Escherichia coli* and thus these were the ones selected to proceed with the respective biochemical and functional characterizations.

### 3.2.1. MQO 1 and MQO 2 from *Staphylococcus aureus*

C41 *E. coli* cells were transformed with plasmids containing the coding gene of MQO 1 *S. aureus* and MQO 2 *S. aureus*. The selected plasmids contained a resistance cassette to kanamycin and thus cell growth was performed in the presence of this antibiotic. The 4L growth was made using Terrific Broth (TB) medium and 100  $\mu$ g/mL of kanamycin (Roth) at 37 °C and at 180 rpm. To induce protein expression, 1 mM of IPTG (Apollo Sientific) was added to the media when cells reached an optical density of 0.6 (OD<sub>600</sub>). After an overnight growth, cells were harvested by centrifugation at 11305 xg, 10 minutes and stored at -20 °C. Samples from this growth collected before and after induction were analyzed by SDS-PAGE to evaluate the expression of the protein. The SDS-PAGE was done as described for the expression tests.

### 3.2.2. MQO from Escherichia coli

*E. coli* Rosetta cells were selected to be transformed with the plasmid containing the gene encoding MQO from *E. coli*. Kanamycin and chloramphenicol were present during the growths due to the resistances of the plasmid and *E. coli* Rosetta cells, respectively.

Cells were grown in Yeast Extract and Tryptone (2YT) medium with 100 µg/mL of kanamycin (Roth) and 34 µg/mL of chloramphenicol (Roth) at 37 °C and 180 rpm, in a 4L growth. Protein expression was induced in the same way as described for *S. aureus* MQO, as well as the cell harvesting and storage. However, in this case the cells were collected 4 hours after induction.

Also, in this case, samples before and after induction were collected and expression of the protein was evaluated by SDS-PAGE. The composition of all solutions and media used to perform expression tests, cell growth and SDS-PAGE gels is presented in Tables 7.1 and 7.2, in appendix.

### 3.3. Protein purification

The initial procedure for the purification of the three proteins, MQO 1 and MQO 2 from *S. aureus* and MQO from *E. coli* was identical. In the three cases, 20 g of cells were resuspended in 50 mM K<sub>2</sub>HPO<sub>4</sub>/KH<sub>2</sub>PO<sub>4</sub> (potassium phosphate) pH 7 (VWR), 300 µg/mL lysozyme (Sigma-Aldrich), 250 mM NaCl (Panreac AppliChem), 10 % glycerol (VWR), containing two complete protease-inhibitor cocktail tablets (Roche). The disruption of cells was performed using a Minilys equipment (Bertin), with three cycles of 45 seconds at the maximum velocity.

Disrupted cells were separated from those non-disrupted by centrifugation at 4100 xg, for 15 minutes. The resulting supernatant was further ultracentrifugated at 204709 xg for 2 hours in order to separate the soluble fraction from the membrane one. The membrane fraction was homogenized in the presence of 50 mM potassium phosphate pH 7 (VWR), 2 M NaCl (Panreac AppliChem), 10 % glycerol (VWR) and one complete protease-inhibitor cocktail tablet (Roche), using a Potter-Evelhjem device. The presence of 2 M NaCl was intended to release the electrostatically interacting membrane proteins, and thus the membrane fraction was incubated in these conditions overnight with agitation at 4° C. In order to separate the released proteins from the membranes, the overnight incubated fraction was ultracentrifugated at 204709 xg, for 1 hour. The ionic strength of the resulting supernatant was decreased to approximately 500 mM, by adding the same buffer without NaCl.

Both soluble and membrane fractions were injected separately in a Histrap High Performance column (5 mL) (GE Healthcare), an affinity column loaded with nickel, which allows a strong interaction with the 6xHisTag from the produced proteins. The column was equilibrated with 50 mM potassium phosphate pH 7 (VWR), 10 % glycerol (VWR), 250 mM NaCl (Panreac AppliChem) and the samples were eluted with a concentration gradient from 0 to 250 mM of Histidines (Roth).

The membrane fraction obtained from the cells expressing the MQO from *E. coli*, and both the soluble and the membrane fractions from the cells expressing MQO 2 from *S. aureus* were further injected in a Q-Sepharose High Performance column (64 mL) (GE Healthcare) because these fractions did not

absorb to the Histrap column. Q-sepharose is an anion exchange column, that separates substances based on their charges using an ion-exchange resin with positively charged groups. The column was equilibrated with 100 mM potassium phosphate pH 7 (VWR) and the samples were eluted with a gradient from 0 to 1 M of NaCl (Panreac AppliChem).

All columns used in the chromatography procedures were connected to an AKTA Prime Plus system (GE Healthcare) and the spectra of the eluted fractions were monitored on a Shimadzu UV-1900 spectrophotometer.

After the chromatography procedures, the samples were concentrated using an Ultra Centrifugal Filter system (Amicon) with a cut-off of 30 kDa.

### **3.4. Protein quantification**

The total protein quantification of the different fractions of MQO 1 and MQO 2 from *S. aureus* and MQO from *E. coli* was determined by Pierce™ Bicinchoninic Acid Protein Assay (BCA) (Thermo Scientific) using Bovine Serum Albumin (BSA) to do a calibration curve, in the range of 0 to 2 mg/mL. The procedure followed the protocol provided by company<sup>32</sup> and absorbances were obtained on a Shimadzu UV-1900 spectrophotometer.

### **3.5. Mass Spectrometry**

The expression and purification of MQO 1 from *S. aureus* was confirmed by mass spectrometry. A SDS-PAGE band with its expected size was analyzed by mass spectrometry at the UniMS, ITQB/IBET.

The data was acquired in positive reflector MS and MS/MS modes using a 5800 plus MALDI TOF/TOF (AB Sciex) mass spectrometer and a TOF/TOF Series Explorer Software v.4.1.0 (Applied Biosystems). External calibration was performed using CalMix5 (Protea).

The identification process used a custom UniProt database with taxonomy restriction to *Staphylococcus aureus*.

### **3.6. Identification of the flavin prosthetic group**

The flavin prosthetic group was identified by reverse phase chromatography. The protein (20 µM MQO 1) was denatured by incubation at 100 °C for 5 min and removed by centrifugation and filtration with a 0.2 µm filter (VWR). Then, the supernatant was injected in a Phenomenex, Luna C18 3 µm (4.6 × 150 mm) column operated in a Dionex Ultimate 3000 HPLC system. The column was equilibrated with Buffer A, 5 mM ammonium sulphate pH 6 and the protein was eluted in the same buffer with an isocratic gradient from 10 to 80 % of Buffer B, methanol (Sigma-Aldrich) at 1 mL/min.

Flavin adenine nucleotide (FAD) (Panreac AppliChem) and Flavin mononucleotide (FMN) (Panreac AppliChem) were also injected in the same column and used as standards.

### 3.7. Determination of the oligomerization state

The oligomerization state of the protein was evaluated by a Native PAGE. The sample, 0.5 µg of MQO 1 from *S. aureus* with sample buffer and Coomassie G250 was loaded onto 4-16 % acrylamide gel and submitted to 160 V, for 1 hour and 20 minutes in an Amersham ECL Gel BOX (Amersham). At the end, the gel was stained with Coomassie G and destained with a destaining solution. The composition of all solutions used is presented in Table 7.2.

### 3.8. Catalytic activity assays

Catalytic activity assays were performed on a Shimadzu UV-1900 spectrophotometer, equipped with a Peltier temperature controlling and a stirring system. The change in absorbance was monitored at 270 nm, the wavelength at which the  $\Delta$ Abs of oxidized and reduced spectra of the DMN is higher (Figure 7.2, in appendix). The reaction solutions were in 50 mM potassium phosphate pH 7 (VWR), 250 mM NaCl (Panreac AppliChem), 10 % glycerol (VWR) in the presence of the scavenging system, a mixture of 5 mM glucose, 4 U ml<sup>-1</sup> glucose oxidase and 130 U ml<sup>-1</sup> catalase to ensure total O<sub>2</sub>-free conditions. Activity assays were done using 3000 µM malate (Sigma-Aldrich) and 100 µM 2,3-Dimethyl-1,4-naphthoquinone (DMN) (Sequoia Research Products), as electron donor and acceptor, respectively, at 37 °C. The reaction mixtures contained 125 nM MQO 1 from *S. aureus*, 250 nM MQO 2 from *S. aureus* or 250 nM MQO from *E. coli*. In the case of MQO 2 from *S. aureus*, the lactate:quinone activity was also tested using 3000 µM of lactate, because there are some studies stating that this protein is a lactate:quinone oxidoreductase instead of a malate:quinone oxidoreductase<sup>27</sup>.

### 3.9. UV-Visible Spectroscopy

All solutions were prepared in 50 mM potassium phosphate pH 7 (VWR), 250 mM NaCl (Panreac AppliChem), 10 % glycerol (VWR) pH 7 buffer in the presence of a scavenging system, as mentioned above. The reduction of MQO was done by the addition of malate (Sigma-Aldrich) in a proportion of 1:100 in the case of MQO 1 from *S. aureus*.

Spectra were collected in a range of wavelengths from 250 to 800 nm, at room temperature on a Shimadzu UV-1900 spectrophotometer.

### 3.10. Steady-state Kinetic Assays

Steady-state Kinetic assays were performed in the same conditions as the catalytic activity assays. The change in absorbance was monitored at the wavelength in which the  $\Delta$ Abs of oxidized and reduced spectra of the quinones is higher (Figure 7.2, in appendix), 278 nm or 270 nm according to the different used quinones, 2,3-Dimethoxy-5,6-dimethyl-p-benzoquinone (DDB) (Sequoia Research Products) or DMN, respectively. All reaction solutions were prepared in 50 mM potassium phosphate pH 7 (VWR), 250 mM NaCl (Panreac AppliChem), 10 % glycerol (VWR) in the presence of the scavenging system mentioned above.

The activity pH profile assays were done between pH 6 and 8.5. The reaction mixture was composed of 3000  $\mu\text{M}$  malate (Sigma-Aldrich), 100  $\mu\text{M}$  DMN and 125 nM MQO 1 from *S. aureus* or 250 nM MQO from *E. coli*.

The kinetic parameters for malate were determined by performing several assays using 100  $\mu\text{M}$  DMN or DDB and varying the concentrations of malate from 100  $\mu\text{M}$  to 3000  $\mu\text{M}$ . The kinetic parameters for the quinones were obtained by performing assays in triplicate using different concentrations of quinones, 5 to 125  $\mu\text{M}$ , and 3000  $\mu\text{M}$  malate (Sigma-Aldrich).

To calculate the protein specific activity ( $\mu\text{mol min}^{-1}\text{mg}^{-1}$ ) the extinction coefficient of the quinones were used, 17545.8  $\text{M}^{-1}\text{cm}^{-1}$  for DMN and 7272.5  $\text{M}^{-1}\text{cm}^{-1}$  for DDB. Michaelis Menten equation,  $V_0 = \frac{V_{\max} [S]}{K_M + [S]}$ , was used to fit the data obtained and the determination of the maximum velocity ( $V_{\max}$ ) and Michaelis Menten constant ( $K_M$ ) was done using a non-linear least-squares regression. The reaction mixture contained 3000  $\mu\text{M}$  malate, 100  $\mu\text{M}$  DMN and 125 nM MQO 1 from *S. aureus*.

### 3.11. Inhibition Assays

To assess the inhibition of the protein's activity, 2-n-Hepthyl-4-hydroxyquinoline-N-oxide (HQNO) (Enzo Life Sciences) was added, in the range from 1 to 100  $\mu\text{M}$ . The reaction mixture contained 3000  $\mu\text{M}$  malate (Sigma-Aldrich), 100  $\mu\text{M}$  DMN and 125 nM MQO 1 from *S. aureus*. The inhibition constant ( $K_i$ )

was determined by the equation,  $V_0 = V_{\max} \frac{(1 + \beta \frac{[I]}{K_i})}{(1 + \frac{[I]}{K_i})}$ .

The assays done to determine the kinetic parameters were repeated in the presence of two concentrations (10 and 20  $\mu\text{M}$ ) of HQNO, in order to determine the inhibition mechanism. The protein specific activity ( $\mu\text{mol min}^{-1}\text{mg}^{-1}$ ) was calculated using the extinction coefficient of the DMN (17545.8  $\text{M}^{-1}\text{cm}^{-1}$ ). The maximum velocity ( $V_{\max}$ ) and Michaelis Menten constant ( $K_M$ ) were determined by fitting the data to the Michaelis Menten equation,  $V_0 = \frac{V_{\max} [S]}{K_M + [S]}$ , and using a non-linear least-squares regression, as for the steady-state kinetic assays.

### 3.12. Fluorescence substrate binding studies

Protein-substrate interaction was evaluated by fluorescence spectroscopy. Fluorescence spectra were obtain using a Fluorolog Jobin Yvon, Horiba and a detector power source TBX-PS.

The reaction mixture, 400  $\mu\text{L}$ , was composed of 2  $\mu\text{M}$  of MQO 1 from *S. aureus* in 50 mM potassium phosphate pH 7 (VWR), 250 mM NaCl (Panreac AppliChem), 10 % glycerol (VWR). Independent titrations were done with each substrate, DMN in the range of 0 to 100  $\mu\text{M}$  and oxaloacetate (Sigma-Aldrich), using concentrations from 100 to 3000  $\mu\text{M}$ . Oxaloacetate was used instead of malate because the protein will oxidize the malate and in this way the data obtained might include not only the effect caused by the binding with the substrate but also the oxidation of the substrate.

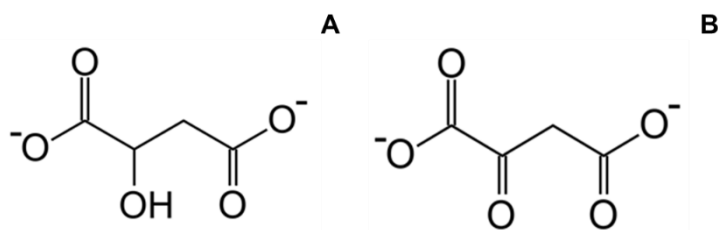


**Figure 3.1-** Chemical structures of malate (A) and oxaloacetate (B).

HQNO was also used, in concentrations between 0 and 125  $\mu\text{M}$ , to titrate the protein and the protein was also titrated with the substrates in the presence of 200  $\mu\text{M}$  of HQNO.

Tryptophan fluorescence emission spectra were obtained at 25° C with an excitation wavelength of 295 nm in the case of DMN and HQNO, and 280 nm in the case of oxaloacetate. The excitation wavelength selected for the DMN was 295 instead of 280 nm, the maximum of the absorption spectrum of tryptophan, because the quinone also absorbs at 280 nm, so we selected a wavelength in which the DMN does not absorb<sup>33,34</sup>. The obtained data were analyzed by normalizing the change in fluorescence at 330 nm due to the addition of each substrate. In order to determine the substrate-enzyme dissociation constants ( $K_D$ ), the obtained data was fitted using the equation  $\Delta F = \frac{\Delta F_{\text{max}} \times [S]}{K_D + [S]}$ .





## 4. Results and Discussion

### 4.1. Biochemical characterization

Malate:quinone oxidoreductases have been the focus of several studies but information on their biochemical characterization is still scarce, specifically due to non-optimized purification processes. In order to obtain considerable amounts of pure protein for structural and functional characterizations, several steps must be carried out, starting by optimization of the expression of the enzyme. In this way several expression tests were performed as described in 3.1.

#### 4.1.1. Expression of MQOs

Expression tests were performed in order to obtain the best conditions for the expression of the gene that codes of each one of the five MQOs studied in this project, MQO 1 and MQO 2 from *S. aureus*, MQO from *E. coli*, MQO from *H. pylori* and MQO from *P. falciparum*. Four different parameters were tested for each protein, the type of expression cells, growth medium, the time of growth after induction and in the case of TB medium, the presence or absence of inducer. Promising results for four of the five proteins under study were obtained, as it is shown in Table 4.1.

**Table 4.1-** Results of the expression tests for the genes coding for the different MQOs. The table shows the conditions tested in the expression tests and respective results. (✓) - Represent the results in which a band with the expected size for each protein was observed in a SDS-PAGE gel.

Cells	Protein	Luria Bertani (LB)*	Yeast Extract and Tryptone (2YT)*	Terrific Broth (TB)	
				With induction	Without induction
<i>E. coli</i> Rosetta	MQO 1 <i>Staphylococcus aureus</i>				
	MQO 2 <i>Staphylococcus aureus</i>				
	MQO <i>Escherichia coli</i>		✓		
	MQO <i>Helicobacter pylori</i>				
	MQO <i>Plasmodium falciparum</i>				
<i>E. coli</i> C43 pLysS	MQO 1 <i>Staphylococcus aureus</i>				
	MQO 2 <i>Staphylococcus aureus</i>				
	MQO <i>Escherichia coli</i>				
	MQO <i>Helicobacter pylori</i>				
	MQO <i>Plasmodium falciparum</i>				
<i>E. coli</i> C41	MQO 1 <i>Staphylococcus aureus</i>			✓	
	MQO 2 <i>Staphylococcus aureus</i>			✓	
	MQO <i>Helicobacter pylori</i>			✓	
	MQO <i>Plasmodium falciparum</i>				

\*In the cases where LB and 2YT media were used, IPTG was always used to induce the protein expression.

In the case of *E. coli* C41 cells, it was not tested the expression of the gene coding for MQO from *E. coli* because it was already found one promising result for the expression of this gene using other cells. The expression of the proteins under study was analyzed by SDS-PAGE gel. The samples tested were collected before the induction with IPTG and at the end of the growth, which in the case of the cells expressing MQO from *E. coli* was four hours after induction and in the other cases was sixteen hours (overnight) after induction. Figure 4.1 shows the respective SDS-PAGE gels indicating the band region with the expected size of each protein.

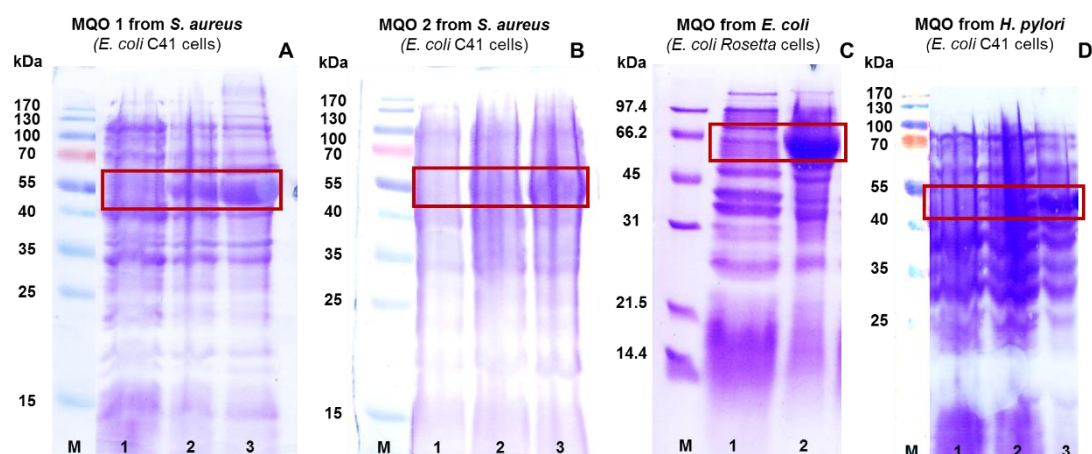


**Figure 4.1-** SDS-PAGE gels of broken cells expressing genes coding for different MQOs. SDS-PAGE gel: Stacking and Resolving Gel – 15 % acrylamide. **A-** MQO 1 from *S. aureus* (molecular mass ~ 57 kDa); **B-** MQO 2 from *S. aureus* (molecular mass ~ 55 kDa); **C-** MQO from *E. coli* (molecular mass ~ 60 kDa); **D-** MQO from *H. pylori* (molecular mass ~ 50.6 kDa); Lane 1: Cells before induction with 1 mM of IPTG; Lane 2: Broken cells 4 hours after induction; Lane 3: Cells 16 hours after induction; M- PeqGold protein marker (**A, B** and **D**) or Low molecular weight (LMW) protein marker (**C**). Red boxes indicate the regions of the protein bands corresponding to the sizes of each MQO.

Among the four genes coding for MQOs that were successfully expressed, MQO from *H. pylori* was not considered to proceed to the next steps, due to time restrictions. The other three enzymes, MQO 1 and MQO 2 from *S. aureus* and MQO from *E. coli*, were used to perform large scale cell growths and proceed to the purification. For that, the conditions revealed to be the best in the expression tests were used for large scale growth (four liters) in order to get a significant quantity of cells for purification. Cell samples obtained before induction and at the end of growth were collected, as in the expression tests, and analyzed by SDS-PAGE to ensure that the gene coding for the protein was being expressed.

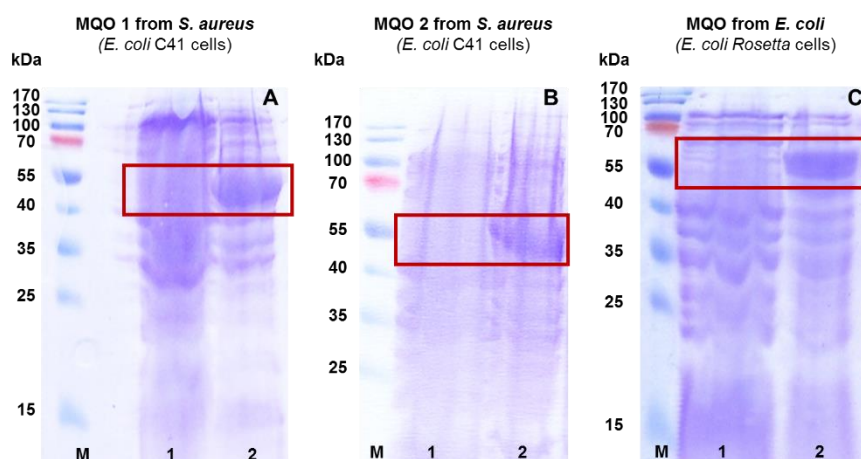


**Figure 4.2-** Expression of three genes coding for MQOs during large scale growths. SDS-PAGE gel: Stacking and Resolving Gel – 15 % acrylamide. **A-** MQO 1 from *S. aureus* (molecular mass ~ 57 kDa); **B-** MQO 2 from *S. aureus* (molecular mass ~ 55 kDa); **C-** MQO from *E. coli* (molecular mass ~ 60 kDa). Lane 1: Broken cells before induction with 1 mM of IPTG; Lane 2: Broken cells 4 hours after induction; M- PeqGold protein marker. Red boxes indicate the regions of the protein bands corresponding to the sizes of each MQO.

In Figure 4.2 we can observe that the gene coding for the protein of interest is being expressed in the three studied cases. Another important aspect for the optimization of the purification process is the cell yield of the growth. In the case of MQO 1 and MQO 2 from *S. aureus* the growth yield was 4 g/L whereas in the case of MQO from *E. coli* it was 2 g/L. After obtaining 100 g of cells expressing each one of the MQOs we proceeded with the purification process.

#### 4.1.2. Purification of MQO 1 and MQO 2 from *S. aureus* and MQO from *E. coli*

The purification process was almost the same for the selected MQOs, MQO 1 and MQO 2 from *S. aureus* and MQO from *E. coli*. After separating membranes from the other cell components by ultracentrifugation, we obtained the soluble fraction that was stored. The resulting membranes were homogenized using a buffer with a high concentration of sodium chloride and incubated overnight. The high salt concentration aims at decreasing the protein-membrane interactions and removing the protein from the membrane. After the incubation another ultracentrifugation was performed from which a membrane fraction (*supernatant*) and membranes (*pellet*) were obtained. The membrane fraction resulted from washing the membranes with 2 M NaCl and thus a decrease in ionic force before injection in an affinity column, an Histrap High Performance 5 mL column, was mandatory.

During the purification process, samples from each step were collected and evaluated by SDS-PAGE to confirm the presence of the protein of interest in all the samples.

##### 4.1.2.1. MQO 1 from *S. aureus*

The purification of MQO 1 from *S. aureus* involved several steps, which were all monitored by SDS-PAGE. Figure 4.3 presents the results of the respective electrophoresis. In lane 1, corresponding to unbroken cells, a band with the expected size (~57 kDa) is observed. This band is as pronounced as the one present in the lane 2 that corresponds to the disrupted cells. One explanation for this result may be the inefficiency of the disrupting cell process. Another hypothesis includes the possibility that the

protein was improperly produced and so inclusion bodies were formed. Inclusion bodies are normally observed in cells that are highly expressing genes coding for recombinant proteins, being very difficult to get the protein of interest from these structures. In this case, the use of chaotropic agents like urea is necessary. In this way, the sample loaded in lane 1 may also be the combination of the two cases, unbroken cells and presence of inclusion bodies.

The homogenization and incubation with 2 M of NaCl was done to extract the protein from the membranes, but the observation of a very intense band with the expected size in lane 6, corresponding to the membranes, suggests that the process was not totally efficient. So, it is possible to conclude that the process to remove the protein from the membranes still needs optimization.

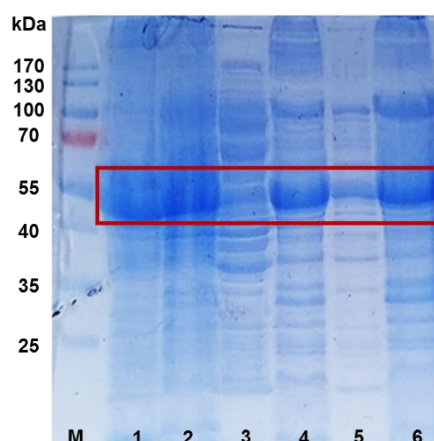


**Figure 4.3-** SDS-PAGE gel of samples from all the steps in the purification of MQO 1 from *S. aureus*. SDS-PAGE gel: Stacking and Resolving gel – 15 % acrylamide. Molecular mass of MQO 1 (*S. aureus*): ~ 57 kDa. Lane 1: Unbroken *E. coli* C41 cells; Lane 2: Broken *E. coli* C41 cells; Lane 3: Soluble fraction; Lane 4: Fraction washed with 2 M of NaCl; Lane 5: Membrane fraction; Lane 6: Membranes; M- PeqGold protein marker. Red box shows the band with the size of MQO 1 from *S. aureus*.

All proteins were expressed with a 6xHisTag, which allows the protein to interact with a metal affinity column. In the case of MQO 1 from *S. aureus* the membrane fraction was injected in a Histrap HP (5 mL) column loaded with  $\text{Ni}^{2+}$ .

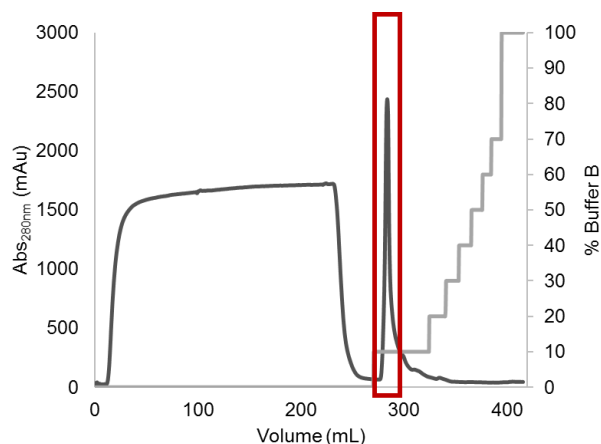


**Figure 4.4-** Chromatogram obtained from the purification of MQO 1 from *S. aureus* using an Histrap HP (5 mL) column. Buffer A: 50 mM potassium phosphate pH 7, 10 % glycerol, 250 mM NaCl; Buffer B: 50 mM potassium phosphate pH 7, 10 % glycerol, 250 mM NaCl, 250 mM Histidines. The dark grey line represents the  $\text{Abs}_{280\text{nm}}$  and in light grey line the % of 250 mM Histidines is represented. Red box corresponds to the MQO 1 from *S. aureus* peak fraction.

Figure 4.4 shows the chromatogram obtained using the Histrap and it is possible to observe that there is only one peak that corresponds to an elution with 10 % of Buffer with histidines (Buffer B).

UV-Visible spectroscopy was performed to evaluate the presence of the protein of interest in the eluted sample, since this protein is a flavoprotein and it has the characteristic spectrum of a flavin, presenting bands with maxima at 375 and 450 nm, as the one showed in Figure 7.2, in the appendix. From the analysis of the UV visible spectra it was possible to confirm the success in the purification of MQO 1 from *S. aureus*.

The collected fraction was concentrated using an Ultra Centrifugal Filter system with a cut-off of 30 kDa and after the sample purity was assessed by SDS-PAGE and a UV-Visible spectrum.

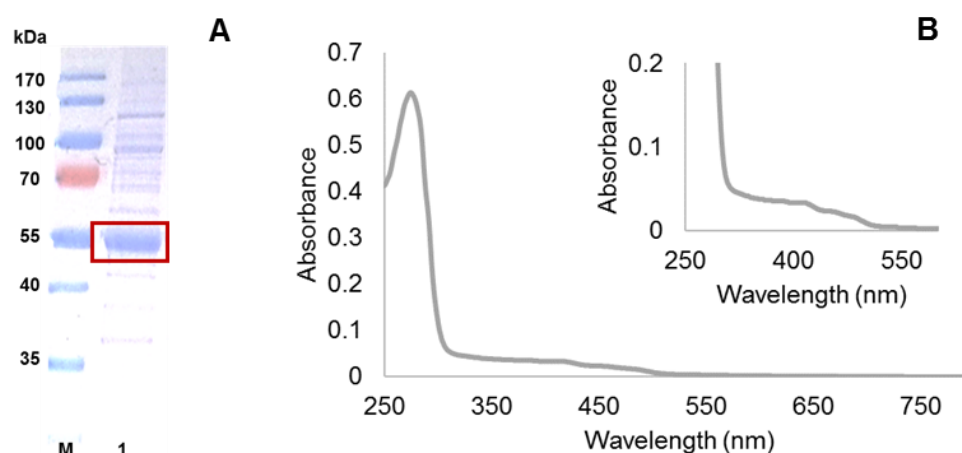


**Figure 4.5-** SDS-PAGE gel and UV-Visible spectrum of the isolated MQO 1 from *S. aureus*. **A-** SDS-PAGE gel of the purified MQO 1 *S. aureus* (molecular mass: ~ 57 kDa) . SDS-PAGE gel: Stacking and Resolving gel – 15 % acrylamide. M- PeqGold protein marker was used; Red box shows the band corresponding to MQO 1 from *S. aureus*. **B-** UV-Visible spectrum of the isolated MQO 1 from *S. aureus* in 50 mM potassium phosphate pH 7, 10 % glycerol, 250 mM NaCl (diluted 1:10). The insert highlights the region between 250 and 550 nm.

It was possible to conclude that the sample was not completely pure because the SDS-PAGE gel (Figure 4.5-A) reveals the presence of other protein bands besides that corresponding to MQO 1 from *S. aureus*. Furthermore, the sample presents an UV visible spectrum characteristic of a flavoprotein with maxima at 375 and 450 nm (Figure 4.5-B) but we also observe another band. This band, around 410 nm, may correspond to the absorption band of a contaminant, cytochrome<sup>35</sup>. Nevertheless, this sample was used for further characterization.

#### 4.1.2.2. MQO 2 from *S. aureus*

Figure 4.6 shows the evaluation of the purification process of MQO 2 from *S. aureus* by SDS-PAGE analyses. Comparing lane 1 and lane 2 is possible to observe in lane 1, that corresponds to the unbroken cells, a band with the expected size (~55 kDa) much more intense than the one corresponding to the broken cells sample (lane 2). This result means that the process of breaking the cells was not completely efficient, as mentioned before in the case of MQO 1. Also, in this case we cannot exclude a possible formation of highly aggregated protein commonly referred to as inclusion bodies.

In addition, as it happened in the case of MQO 1 from *S. aureus*, in lane 6, corresponding to the membranes, there is a band with the expected size. So, this part of the purification process from membranes that includes the homogenization and incubation with NaCl still needs optimization in order to obtain higher amounts of protein.

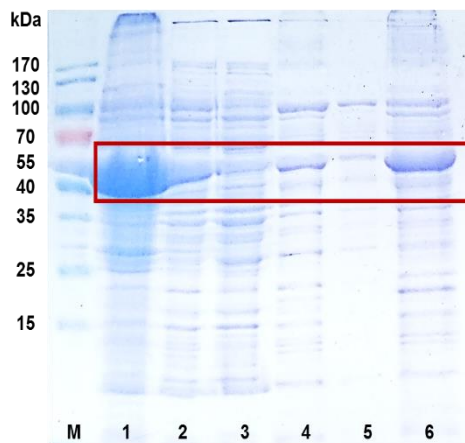


**Figure 4.6-** SDS-PAGE gel with the samples from all the steps in MQO 2 from *S. aureus* purification process. SDS-PAGE gel: Stacking and Resolving Gel – 15 % acrylamide. Molecular mass of MQO 2 (*S. aureus*): ~ 55 kDa; Lane 1: Unbroken *E. coli* C41 cells; Lane 2: Broken *E. coli* C41 cells; Lane 3: Soluble fraction; Lane 4: Fraction washed with 2 M of NaCl; Lane 5: Membrane fraction; Lane 6: Membranes; M- PeqGold protein marker. Red box shows the band with the size of MQO 2 from *S. aureus*.

For the purification of MQO 2 from *S. aureus*, both soluble and membrane fractions were selected to be injected in the Histrap HP (5 mL) column. Contrary to the case of MQO 1 from *S. aureus*, in lane 5, which corresponds to the membrane fraction, it is possible to observe a very thin band around 55 kDa. In order to obtain high amounts of purified protein and since the band was also present in the soluble fraction, represented in lane 3, this fraction was also injected in the same column. The chromatograms corresponding to the injection of both the soluble and the membrane fractions of MQO 2 from *S. aureus* are shown in Figure 4.7.

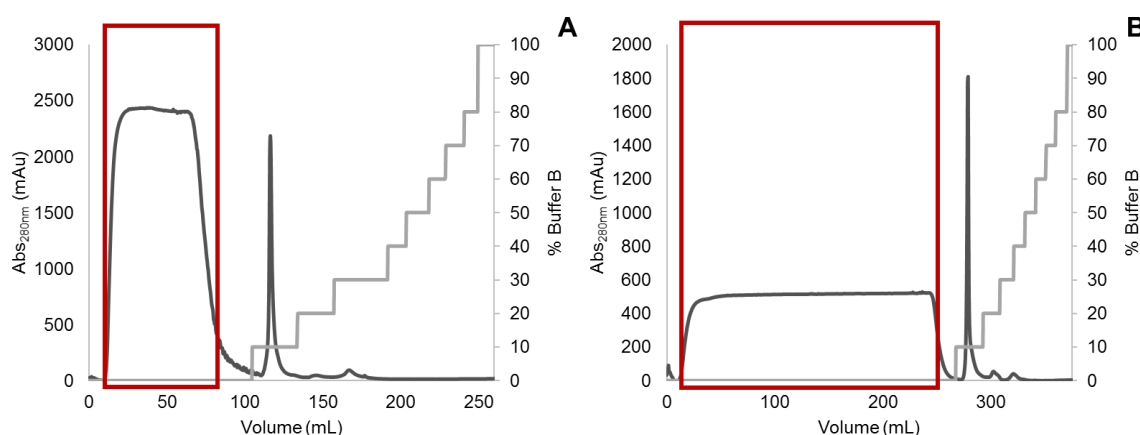


**Figure 4.7-** Chromatograms obtained from the purification of MQO 2 from *S. aureus* using an Histrap HP (5 mL). **A-** Chromatogram obtained with the injection of soluble fraction of MQO 2 from *S. aureus*; **B-** Chromatogram obtained by the injection of membrane fraction of MQO 2 from *S. aureus*; Buffer A: 50 mM potassium phosphate pH 7, 10 % glycerol, 250 mM NaCl; Buffer B: 50 mM potassium phosphate pH 7, 10 % glycerol, 250 mM NaCl, 250 mM Histidines. The dark grey line represents the Abs<sub>280nm</sub>, in light grey line the % of 250 mM Histidines is represented. Red boxes correspond to MQO 2 from *S. aureus* elution.

The analysis by UV-Visible spectroscopy of each sample from the two chromatographic procedures showed that the protein did not adsorb to the column, because the samples that showed a characteristic spectrum of a flavoprotein were the ones present in the beginning of the chromatogram. This means that the samples injected in the columns did not adsorb to it. This situation can occur in cases where the 6xHisTag is not exposed to the matrix of the column and in this way the protein is not able to interact with it.

To further attempt to purify MQO 2 from *S. aureus*, we decided to inject the protein in a Q-Sepharose High Performance (64 mL) column. This column was selected because it is used in the host lab to purify other monotopic proteins and it is an anion exchange column that separates proteins according to their charges. Considering the principle of this column, if the sample has a high ionic strength it will not adsorb to the column because the ions present in the sample will interact more strongly with the column than the protein. This means that we had to decrease the ionic strength of both soluble and membrane fractions. In the case of the soluble fraction, it was possible to decrease the ionic strength by adding a buffer such as Buffer A used for the Histrap column but without NaCl because the ionic strength was lower than in the case of the membrane fraction for which we had to do a dialysis. Afterwards, the samples with the correct ionic strength were injected in the Q- Sepharose HP (64 mL) column.

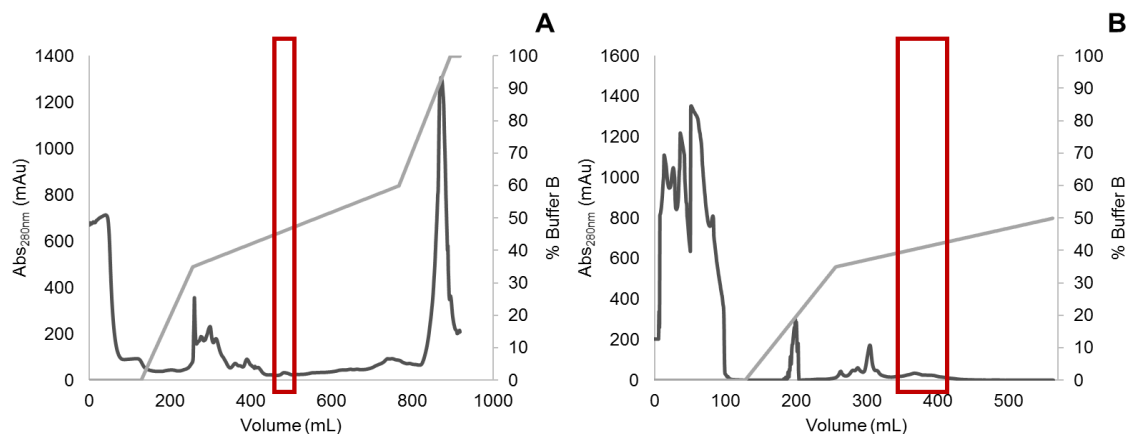


**Figure 4.8-** Chromatograms obtained from the purification of MQO 2 from *S. aureus* using a Q- Sepharose HP (64 mL) column. **A-** Chromatogram obtained with the injection of soluble fraction of MQO 2 from *S. aureus*; **B-** Chromatogram obtained by the injection of membrane fraction of MQO 2 from *S. aureus*; Buffer A: 100 mM potassium phosphate pH 7; Buffer B: 100 mM potassium phosphate pH 7, 1 M NaCl. The dark grey line represents the Abs<sub>280nm</sub>, in light grey line the % of 1 M NaCl is represented. Red boxes correspond to MQO 2 from *S. aureus* elution.

Figure 4.8-A/B presents the chromatograms for the purification of both soluble and membrane fractions of MQO 2 from *S. aureus* and it is possible to observe that the proteins in each fraction were separated. Analyzing the UV-Visible spectra of the eluted samples it was possible to confirm the presence of MQO 2 from *S. aureus* in both fractions since the spectrum typical of a flavoprotein was observed. The elution of MQO 2 from *S. aureus* took place with 40 % of Buffer with NaCl (B) in both soluble and membrane fractions. The MQO 2 from *S. aureus* purified from the soluble fraction was designated Fraction A and the protein purified from the membrane fraction, Fraction B.



Fractions A and B were concentrated using the same system as the one used for MQO 1 from *S. aureus*. In order to assess the purity of the samples, these were analyzed by SDS-PAGE and UV-Visible spectroscopy (Figure 4.9).

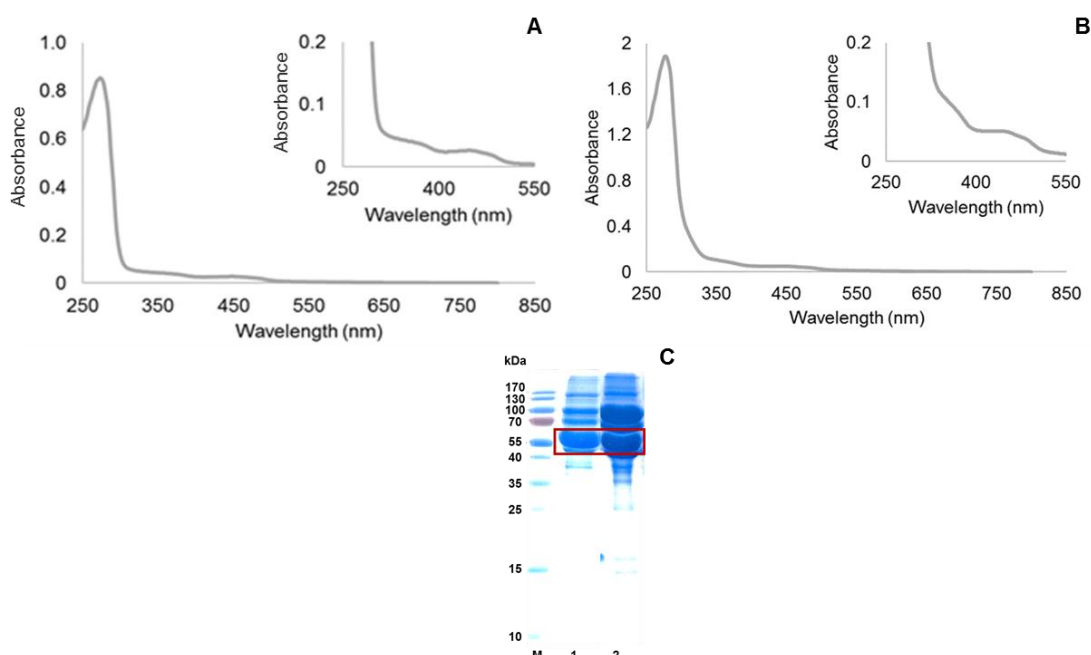


**Figure 4.9-** UV-Visible spectra and SDS-PAGE gel of the isolated MQO 2 from *S. aureus*. **A-** UV-Visible spectrum of Fraction A; **B-** UV-Visible spectrum of Fraction B; Samples in 50 mM potassium phosphate pH 7, 10 % glycerol, 250 mM NaCl. The figures show a zoom of the region between 250 and 550 nm; **C-** SDS-PAGE gel of the purified MQO 2 *S. aureus* (molecular mass: ~ 55 kDa); SDS-PAGE gel: Stacking and Resolving Gel – 15 % acrylamide; Lane 1- Fraction B; Lane 2- Fraction A; M- PeqGold protein marker. Red box shows the band corresponding to MQO 2 from *S. aureus*.

The spectra of Fraction A (Figure 4.9-A) and Fraction B (Figure 4.9-B) are typical of flavoproteins, having the characteristic bands with maxima at 375 and 450 nm. Beyond this, looking at Figure 4.9-C, the SDS-PAGE gel shows that there are more bands than the one corresponding to MQO 2 *S. aureus*. Taking these two observations into account, we can conclude that despite the fractions having the characteristic spectra of a flavoprotein, the SDS-PAGE gel shows the presence of other proteins. Nonetheless, we decided to continue the characterization of these samples and test malate:quinone oxidoreductase activity.

#### 4.1.2.3. MQO from *E. coli*

The purification of MQO from *E. coli* followed the same procedure as that of MQO 2 from *S. aureus*, although the protein was purified only from the membrane fraction. Figure 4.10 shows all the samples of MQO from *E. coli* along the purification process, evaluated by SDS-PAGE. As in the case of the other two proteins (MQO 1 and MQO 2 from *S. aureus*) it is possible to observe a band with the expected size (~60 kDa) in all lanes, including lane 5, which corresponds to the membranes. This means once again that the extraction process from the membranes was not completely efficient and still needs optimization.



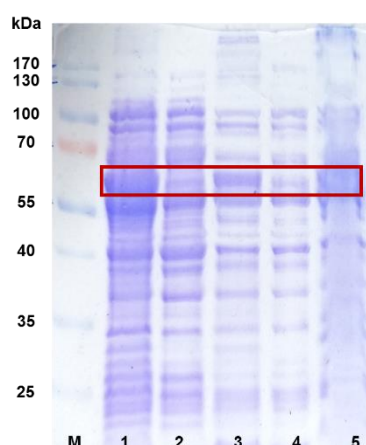


**Figure 4.10-** SDS-PAGE gel of the samples from all the steps of MQO from *E. coli* along the purification process. SDS-PAGE gel: Stacking and Resolving Gel – 15 % acrylamide. Molecular mass of MQO (*E. coli*): ~ 60 kDa; Lane 1: Broken *E. coli* Rosetta cells; Lane 2: Soluble fraction; Lane 3: Fraction washed with 2 M of NaCl; Lane 4: Membrane fraction; Lane 5: Membranes; M- PeqGold protein marker. Red box shows the band with the size of MQO from *E. coli*.

In Figure 4.10 it is possible to observe that in lanes 2 and 4, corresponding to soluble and membrane fractions, respectively, there is a tiny band with the expected size, so both fractions were injected in the Histrap HP (5 mL) column.

The chromatograms corresponding to the injection of both soluble and membrane fractions of MQO from *E. coli* in the Histrap column are shown in Figure 4.11.

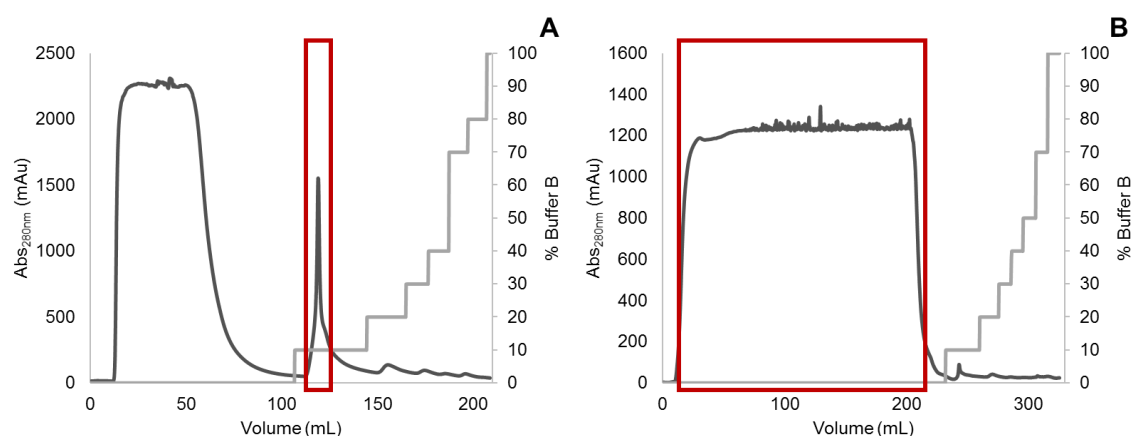


**Figure 4.11-** Chromatogram obtained from the purification of MQO from *E. coli* using an Histrap HP (5 mL) column. **A-** Chromatogram obtained with the injection of soluble fraction of MQO from *E. coli*; **B-** Chromatogram obtained by the injection of membrane fraction of MQO from *E. coli*; Buffer A: 50 mM potassium phosphate buffer pH 7, 10 % glycerol, 250 mM NaCl; Buffer B: 50 mM potassium phosphate pH 7, 10 % glycerol, 250 mM NaCl, 250 mM Histidines. The dark grey line represents the Abs<sub>280nm</sub>, in light grey line the % of 250 mM Histidines is represented. Red boxes correspond to MQO from *E. coli* elution.

Figure 4.11-A presents the chromatogram obtained from the injection of the soluble fraction in the Histrap HP (5 mL) column. It is possible to observe that there is one peak corresponding to an elution with 10 % of Buffer with histidines (Buffer B). As in the other cases, UV-Visible spectroscopy was used to confirm the presence of the protein of interest in the eluted sample. The analysis of the UV visible spectra showed that this collected sample is a flavoprotein. This fraction was designated Fraction A.

Figure 4.11-B shows the chromatogram of the membrane fraction of MQO from *E. coli*. The analysis by UV-Visible spectroscopy showed that the protein did not adsorb to the column, because the samples with the characteristic spectrum of a flavoprotein, were those that eluted first. This result means that the protein did not adsorb to the column which can happen when the tag is not exposed.

As the membrane fraction did not adsorb to the Histrap column, we decided to inject it in a Q-Sepharose High Performance (64 mL) column, an anion exchange column. As previously explained, we had to decrease the ionic strength due to the interaction between the column and the ions present in the sample. To decrease the ionic strength a dialysis, against a buffer such as Buffer A used for the Histrap column but without NaCl, was done before injecting the sample in the Q- Sepharose HP (64 mL) column.

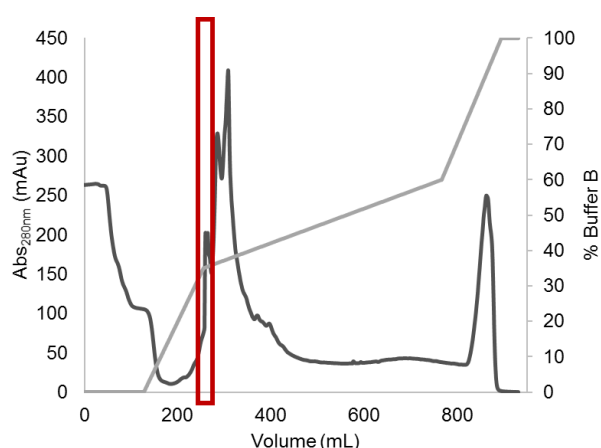


**Figure 4.12-** Chromatogram obtained from the purification of membrane fraction of MQO from *E. coli* using a Q-Sepharose HP (64 mL) column. Buffer A: 100 mM potassium phosphate pH 7; Buffer B: 100 mM potassium phosphate pH 7, 1 M NaCl, pH 7. The dark grey line represents the Abs<sub>280nm</sub>, in light grey line the % of 1 M NaCl is represented. Red box corresponds to MQO from *E. coli* elution.

Figure 4.12 presents the chromatogram for the purification of the membrane fraction of MQO from *E. coli*. This chromatogram shows that it was possible to separate the proteins present in the injected fraction since there are different peaks at different elution volumes. After the analysis of the UV-Visible spectra of the eluted samples it was possible to confirm the presence of MQO from *E. coli* in one sample that had the characteristic spectrum of a flavoprotein. The elution of this sample was with 35 % of Buffer with NaCl (Buffer B) and this sample was designated Fraction B.

Fraction A, eluted from the Histrap column, and Fraction B obtained using the two columns mentioned above, were concentrated using the same system as the one used for MQO 1 and 2 from *S. aureus*. In order to assess the purity of the samples, SDS-PAGE and UV-Visible spectroscopy were performed (Figure 4.13).

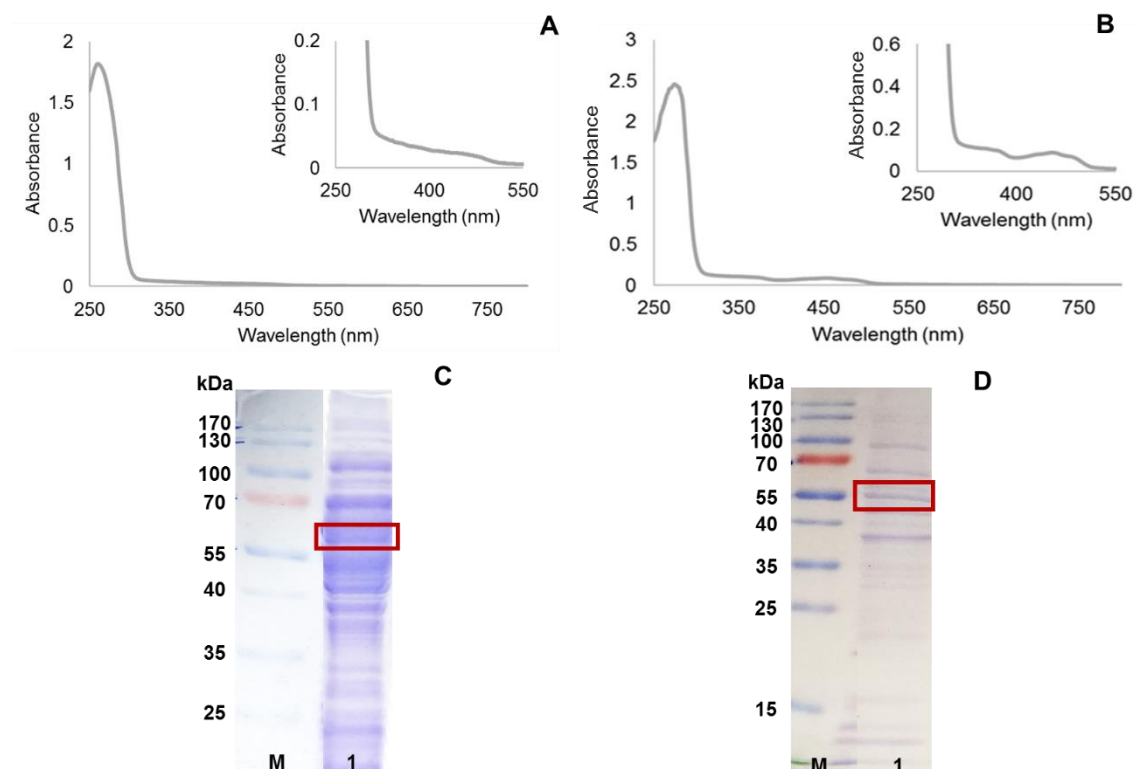


**Figure 4.13-** UV-Visible spectra and SDS-PAGE gel of the purified MQO from *E. coli*. **A-** UV-Visible spectrum of Fraction A (diluted 1:10); **B-** UV-Visible spectrum of Fraction B; Samples in 50 mM potassium phosphate pH 7, 10 % glycerol, 250 mM NaCl. The figures show a zoom in the region between 250 and 550 nm; **C-** SDS-PAGE gel of Fraction A (MQO from *E. coli*); **D-** SDS-PAGE gel of Fraction B (MQO from *E. coli*); Molecular mass of MQO (*E. coli*): ~ 60 kDa; SDS-PAGE gel: Stacking and Resolving Gel – 15 % acrylamide. M- PeqGold protein marker. Red boxes show the band corresponding to MQO from *E. coli*.

Figure 4.13-A/B shows the spectra of the two purified fractions of MQO from *E. coli* where it is possible to observe that the spectrum of Fraction B is characteristic of a flavoprotein (bands with maxima at 375 and 450 nm). The spectrum of Fraction A also has the same characteristic bands but with less protein since the peaks are not so pronounced as in the spectrum of Fraction B.

In addition to the UV-Visible spectra, SDS-PAGE gels of the purified samples were done (Figure 4.13-C/D). In Fraction A (Figure 4.13-C) it is possible to observe that this fraction is not pure. Besides the band with the expected size there are other bands, showing that this fraction has other proteins. The SDS-PAGE gel of the other purified fraction (Fraction B) shows few bands with the band of interest with the expected size. The purified fractions were further characterized.

#### 4.1.3. Protein quantification

At the end of the purification process for the three MQOs, the purified protein was quantified using the Bicinchoninic Acid Protein Assay Kit. This kit quantifies the total amount of protein in the samples using a BSA protein as a standard.

For each MQO that was isolated, we selected one sample based on the respective SDS-PAGE results and UV-Visible spectrum. The selected samples were quantified not only in terms of total protein but also in terms of the flavin content, since the protein of the interest is a flavoprotein. The absorbance at

450 nm was used to calculate the concentration of flavin using the Lambert-Beer law<sup>36</sup>. The obtained quantification values are reported in Table 4.2.

**Table 4.2-** Quantification of total protein and flavin content of the samples of MQO 1 and MQO 2 from *S. aureus* and MQO from *E. coli*.

	MQO 1 <i>S. aureus</i>	MQO 2 <i>S. aureus</i>	MQO <i>E. coli</i>
Total protein (mg/mL)	5.43	8.59	9.31
[Flavin] (mg/mL)	1.16	0.43	1.12

We observed that MQO 1 from *S. aureus* is the one presenting the best flavin/total protein ratio (ratio: 1/5). These results agree with those from SDS-PAGE and UV visible spectroscopy already discussed. Indeed, the fractions of MQO 2 from *S. aureus* and MQO from *E. coli* showed the presence of more contaminants than the fraction of MQO 1 from *S. aureus*, confirming the ratios obtained and presented in Table 4.2. Accordingly, the flavin content (Table 4.2) is higher in the cases of MQO 1 from *S. aureus* and MQO from *E. coli* than for MQO 2 from *S. aureus*.

#### 4.1.4. Protein identification

In order to confirm the identity of the isolated protein, the band with the size corresponding to that of MQO 1 from *S. aureus* (~57 kDa) present in the SDS-PAGE gel (Figure 4.5) was analyzed by mass spectrometry at the UniMS IBET/ITQB. As the protein under study is from *Staphylococcus aureus*, the database used had a taxonomy restriction to this microorganism. The protein band analyzed was identified, with 49 % of sequence coverage, as Probable malate:quinone oxidoreductase (assay report in Figure 7.2, appendix).

#### 4.1.5. Identification of the flavin prosthetic group

A flavoprotein, as described above, may contain FAD, FMN or other types of flavin as prosthetic group. However, by UV-Visible spectroscopy, it is not possible to distinguish between them because both compounds have similar spectra with maxima at 375 and 450 nm. In order to determine which of the flavin prosthetic group MQO 1 from *S. aureus* contains, a reverse phase chromatography was performed.

Commercial FAD and FMN were used as standards, being injected to the column to obtain the retention time of each prosthetic group. After that, a sample with the flavin prosthetic group of the MQO 1 from *S. aureus*, was injected to the same column. In this way we could compare the retention time and determine which prosthetic group was present in the sample of MQO 1 from *S. aureus*. The retention times of the three samples are presented in the Table 4.3.

**Table 4.3-** Retention times of the flavin prosthetic groups. Retention times of the standards (FAD and FMN) and sample injected in a reverse phase column operated in a HPLC system.

Sample	Retention time (mL)
FAD	12.0
FMN	12.7
MQO 1 from <i>S. aureus</i>	12.0

The retention times present in Table 4.3 show that the sample with the prosthetic group of MQO 1 from *S. aureus* has the same retention time as the FAD sample. This result means that MQO 1 from *S. aureus* has a FAD as a prosthetic group.

#### 4.1.6. Oligomerization state of MQO

The oligomerization is a process that associates monomers in non-covalently bound macromolecular complexes. There are experimental evidences that MQOs from other organisms are present in different oligomerization states, so we decided to determine the oligomerization state of MQO 1 from *S. aureus*. For that, a Blue Native PAGE was done using the purified sample of MQO 1 from *S. aureus*.

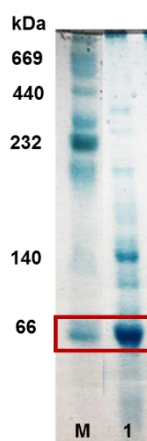


**Figure 4.14-** Blue Native PAGE gel with MQO 1 from *S. aureus* (molecular mass: ~ 57 kDa); Acrylamide gel- 4 a 16 %; M- Marker for Native PAGE. Red box shows the band corresponding to MQO 1 from *S. aureus*.

The gel in the Figure 4.14 shows a very pronounced band with a molecular mass around 66 kDa. This band may correspond to MQO 1 from *S. aureus*, which has a molecular mass around 57 kDa. Considering that the gel has an inherent error that can explain the difference between the molecular masses, it is possible to conclude that the protein is predominantly a monomer.

It is also possible to observe that the gel has more bands than the one corresponding to MQO 1 from *S. aureus*, which can be explained by the impurity of the sample, already observed in the SDS-PAGE

gel. The other explanation for this is that the protein can be in different oligomerization states in solution (Figure 4.5), a dimer in this case.

## 4.2. Functional Characterization

The functional characterization of proteins is just as important as the biochemical characterization. The results obtained for the biochemical characterization allowed us to proceed to the functional characterization in which we aimed to explore the catalytic mechanism of these enzymes and their interaction with both substrates, malate and quinone.

### 4.2.1. Catalytic activity assays

Malate:quinone oxidoreductase activity assays were performed for the three purified proteins using both substrates, malate and quinone (DMN). In addition, the possibility that MQO 2 from *S. aureus* uses lactate instead of malate was also tested, as it has been suggested that this protein may be a lactate:quinone oxidoreductase (LQO). The absence of oxygen in the reaction was guaranteed by the presence of the so-called scavenging system, a mixture composed of two enzymes (glucose oxidase and catalase) and glucose that consumes all the oxygen present in the reaction mixture reducing it to water (Figure 7.3, in appendix).

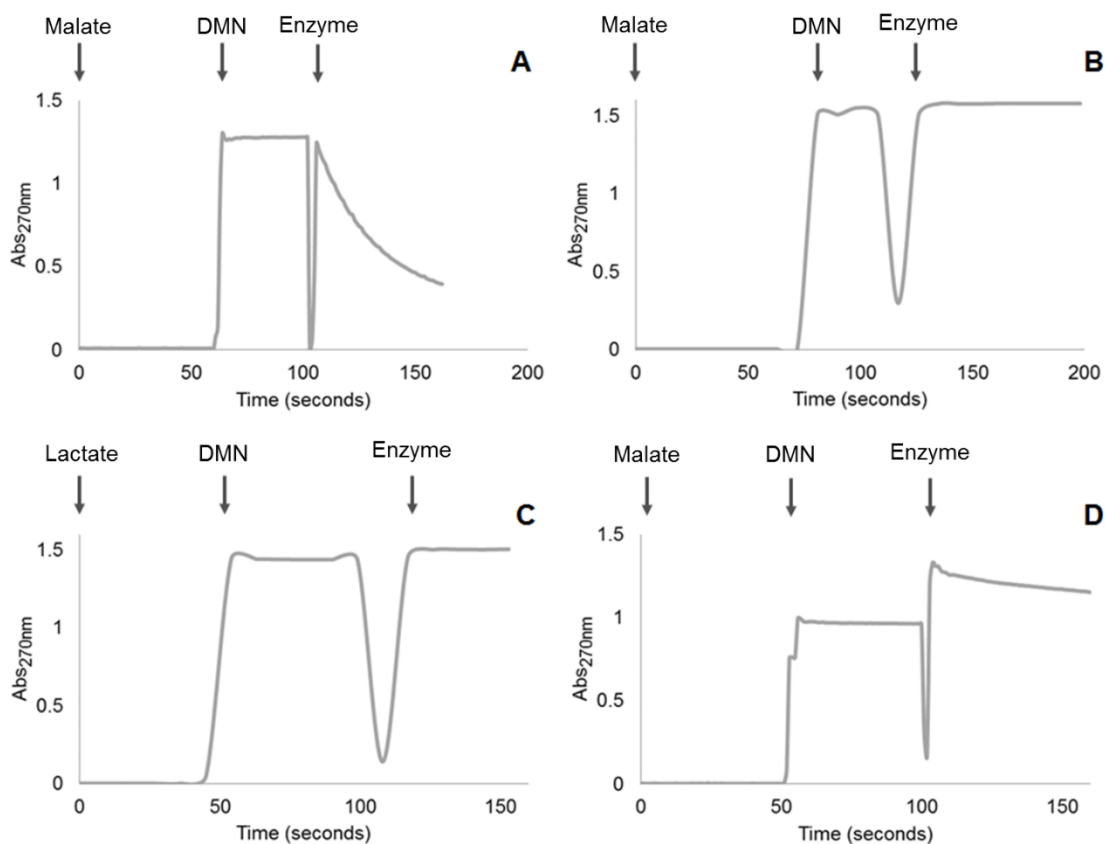


**Figure 4.15-** Catalytic activity assays with MQO 1 from *S. aureus* (A), MQO 2 from *S. aureus* (B and C) and MQO from *E. coli* (D). Assays done in aerobic conditions, using scavenging system, at 37 °C in 50 mM potassium phosphate pH 7, 10 % glycerol, 250 mM NaCl.

Figure 4.15 shows the catalytic activity assays, following the change in absorbance of DMN at 270 nm. As expected, the absorbance of DMN decreases when the protein is added to the assay since quinone is reduced to quinol.

In the case of MQO 1 from *S. aureus* (Figure 4.15-A) we observed a pronounced slope after the addition of the protein, meaning that the protein has malate:quinone oxidoreductase activity. Figure 4.15-B shows the activity assay using MQO 2 from *S. aureus* where we did not observe a decrease in the absorbance at 270 nm, which means that the protein did not use the given substrates, malate and DMN. This result was not totally unexpected because there are some studies stating that this protein might be a lactate:quinone oxidoreductase (LQO), instead of a malate:quinone oxidoreductase. In this way, we performed an activity assay changing malate for lactate (Figure 4.15-C), but again we did not observe a decrease in the absorbance at 270 nm. These results revealed that the purified MQO 2 from *S. aureus* was not active in the conditions tested, so it is necessary to test other conditions to determine which are the best conditions for MQO 2 from *S. aureus* being active. It is also important to keep in mind that the protein was not identified by mass spectrometry, so there is a possibility that the purified protein may not be MQO 2 from *S. aureus* and, in this case, it is necessary to optimize the expression conditions. Concerning MQO from *E. coli* we observed a decrease in the absorbance at 270 nm, meaning that this enzyme has malate:quinone oxidoreductase activity, as MQO 1 from *S. aureus* (Figure 4.15-D).

Considering these results, MQO 1 from *S. aureus* and MQO from *E. coli* were selected to proceed with the functional characterization.

#### 4.2.2. Enzymatic activity pH profile

Enzymatic activity can be affected by a variety of factors, such as temperature, protein and substrates concentration and pH. Each enzyme has an optimal pH range and changing the pH outside of this range will slow the enzyme activity. In addition, extreme pH values can cause the denaturation of proteins and for that reason the pH is also an important factor in the stability of enzymes. In order to determine the optimal pH of MQO 1 from *S. aureus* and of MQO from *E. coli*, a pH profile for each one was performed. Experiments were done under O<sub>2</sub>-free conditions, guaranteed by the scavenging system, at 37 °C, varying the pH values from pH 6 to pH 8. The activity of the proteins was obtained by following the change in absorbance of DMN at 270 nm, malate was used as electron donor and quinone the electron acceptor. The pH profiles for both proteins are presented in Figure 4.16.

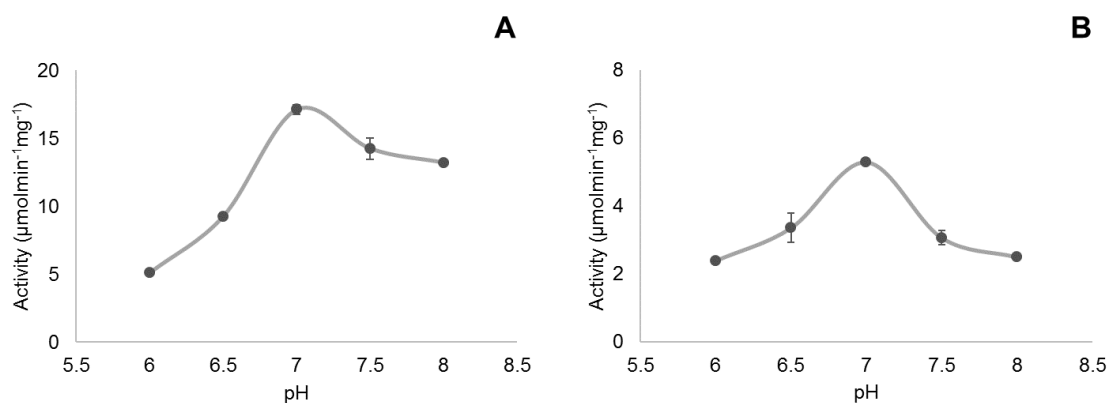


**Figure 4.16-** pH profile of MQO 1 from *S. aureus* (A) and of MQO from *E. coli* (B). Assays were performed under anaerobic conditions, using scavenging system, at 37 °C, in 50 mM potassium phosphate, 10 % glycerol, 250 mM NaCl pH values between 6 and 8. Each point, presented with error bars, corresponds to duplicate experiments using 100  $\mu\text{M}$  DMN, 3000  $\mu\text{M}$  malate and 125 nM of MQO 1 from *S. aureus* or 250 nM of MQO from *E. coli*.

The highest activities for both enzymes were obtained at pH 7 which is consistent with the cytoplasmic pH of these microorganisms<sup>37,38</sup> (Figure 4.16).

#### 4.2.3. Reduction of MQO

An oxidation:reduction (redox) reaction is a type of chemical reaction that involves a transfer of electrons between two species. The reaction catalyzed by MQO is a redox reaction, since there is an oxidation of malate that reduces the FAD, involving the transfer of electrons and a reduction of the quinone that subsequently re-oxidizes  $\text{FADH}_2$ . To determine if this protein is redox active, UV-Visible spectroscopy was used. The spectra were done in the presence of the scavenging system to deplete oxygen in solution.

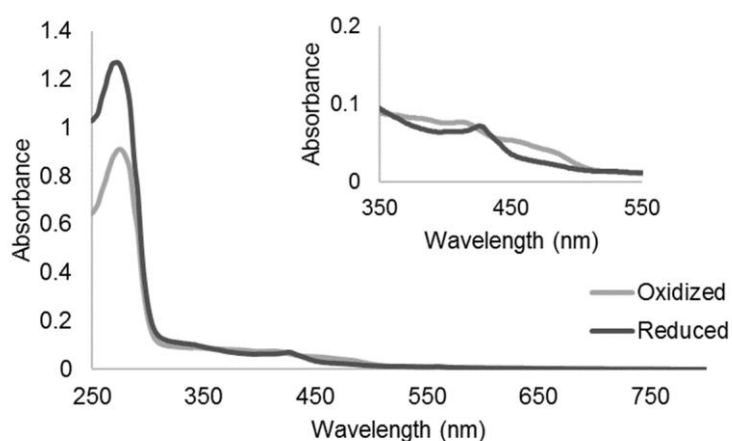


**Figure 4.17-** UV-Visible spectrum of MQO 1 from *S. aureus* oxidized (light grey) and reduced (dark grey) with 1000  $\mu\text{M}$  malate, in 50 mM potassium phosphate pH 7, 10 % glycerol, 250 mM NaCl. Spectra were obtained under anaerobic conditions ensured by the scavenging system, 37 °C using 10  $\mu\text{M}$  MQO1 from *S. aureus*. The inserted figure expands absorption spectrum in the 250–550 nm region.



Figure 4.17 shows the spectra of the oxidized and the reduced states of MQO 1 from *S. aureus*. The oxidized form presents a spectrum showing the characteristic bands with maxima at 375 and 450 nm of a flavoprotein, already seen in Figure 4.5.

To reduce the protein, malate was added in a proportion of 1:100 and as can be observed in the Figure, the reduced state is characterized by the loss of absorption in the 375-450 nm region. We also attempted to re-oxidize the protein by adding the quinone, DMN, but it was impossible to observe the oxidation of the enzyme since DMN was in a very high concentration (1:100) and its addition leads to protein precipitation.

#### 4.2.4. Steady-state Kinetic Assays

The catalytic mechanism of an enzyme is the process of using a specific substrate and transforming it into products. To understand the catalytic mechanism, we investigated the kinetics of the enzyme by using the best-known model of enzyme kinetics, the Michaelis-Menten model. The Michaelis-Menten model is used to predict the rate of product formation and is defined by an equation that describes the rate of enzymatic reactions, considering the reaction rate and the concentration of the substrate. In this equation,  $V_0 = \frac{V_{max} [S]}{K_M + [S]}$ , where  $V_{max}$  represents the maximum rate achieved by the enzyme and the  $K_M$  is the Michaelis-Menten constant defined by the substrate concentration that the enzyme needs to reach half of the maximum rate. This model is used to explain the reactions that occur between an enzyme and a substrate, but it can be also used for multi-substrate reactions if we keep constant the concentration of one of the substrates and vary the concentration of the other one. In this case, the enzyme will behave as a single substrate enzyme and we can determine the parameters of each substrate individually.

Considering that, steady-state kinetic assays using MQO 1 from *S. aureus* and MQO from *E. coli* were done varying the concentrations of one substrate and keeping the other one constant, in order to determine the kinetic parameters for each MQO. In the case of MQO from *E. coli*, the experiments were also performed using another quinone, DDB, because *E. coli* can synthesize both quinones depending on the growth conditions (aerobic or anaerobic) and we wanted to investigate if there was any difference in the activity by using different quinones. The results of these assays are shown in Figure 4.18, in which the values were obtained from two independent assays and the respective error bars are also represented.

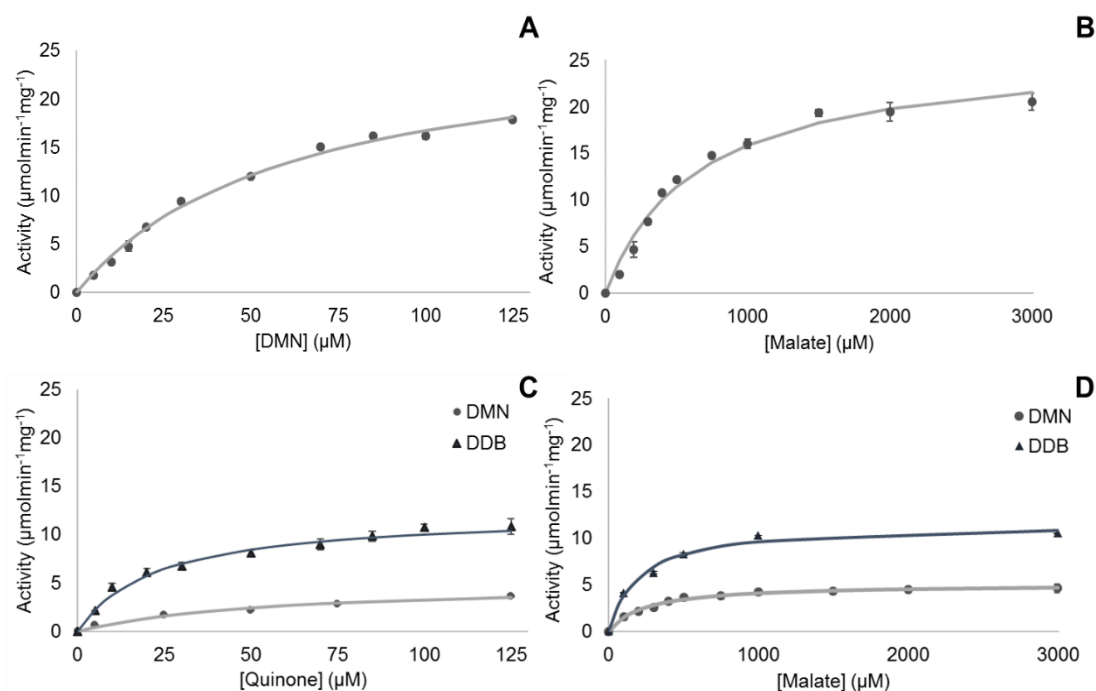


**Figure 4.18-** Steady-state analyses of MQO 1 from *S. aureus* and of MQO from *E. coli*. Malate:quinone oxidoreductase activity as function of the concentration of DMN (A) or malate (B) using 125 nM MQO 1 from *S. aureus*. Malate:quinone oxidoreductase activity as function of the concentration of DMN or DDB (C) or malate (D) using 250 nM MQO from *E. coli*. The data points were fitted with a Michaelis-Menten equation (full line),  $V_0 = (V_{\max} [S]) / (K_M + [S])$ . All the assays were done under anaerobic conditions, using a scavenging system, at 37 °C in 50 mM potassium phosphate pH 7, 10 % glycerol, 250 mM NaCl.

Figure 4.18 describes a dependency on the substrate for both MQOs, the increase in the substrate concentration increases the activity of the protein until it reaches the maximum velocity. At this stage, the increase of the substrate's concentration does not affect the maximum velocity. This behavior is characteristic of a Michaelis-Menten mechanism.

In the case of MQO 1 from *S. aureus*, the  $V_{\max}$  values determined from the curves in Figure 4.18-A/B, were  $27.0 \pm 0.6$  and  $26.1 \pm 0.1 \mu\text{mol min}^{-1}\text{mg}^{-1}$  while the  $K_M$  values were  $61.4 \pm 3.8$  and  $646.5 \pm 9.0 \mu\text{M}$ , for DMN and malate, respectively (Table 7.3, in appendix). Malate has a higher  $K_M$  value than the DMN, meaning that the enzyme needs more amount of malate for the reaction to occur. The  $K_M$  value is an inverse measure of the substrate's affinity for the enzyme, if the  $K_M$  value is higher, it means that the protein has less affinity for that substrate. So, in the case of MQO 1 from *S. aureus*, we can conclude that the protein has more affinity for DMN than for malate, since it has a lower  $K_M$  value than for DMN. For MQO from *E. coli*, the kinetic parameters were first determined for the two quinones, DMN and DDB (Figure 4.18-C), the number of points in each curve is different due to the available amount of protein. The  $V_{\max}$  values were  $5.0 \pm 0.2$  and  $12.3 \pm 0.2 \mu\text{mol min}^{-1}\text{mg}^{-1}$  and the  $K_M$  values were  $53.1 \pm 3.4$  and  $22.7 \pm 1.5 \mu\text{M}$ , for DMN and DDB, respectively (Table 7.4, in appendix). Considering the  $V_{\max}$  values, we observe that the protein reaches a higher activity when it uses DDB and this observation is confirmed by the  $K_M$  values, since the  $K_M$  value for DDB is lower than the one for DMN. This result is in agreement

to our previous work since all the growths were performed in aerobiosis and *E. coli* only expresses DDB in aerobic conditions, this quinone being the preferred one.

The enzyme also showed a Michaelis-Menten behavior toward malate where the kinetic constants were also determined in the presence of both quinones (Figure 4.18-D). The  $V_{max}$  values were  $5.1 \pm 0.2$  and  $11.6 \pm 0.0 \mu\text{mol min}^{-1}\text{mg}^{-1}$  while the  $K_M$  values were  $242.0 \pm 21.4$  and  $202.1 \pm 9.9 \mu\text{M}$  in the presence of DMN and DDB, respectively (Table 7.5, in appendix). These results show that the maximum velocity is affected differently by the two quinones, since the  $V_{max}$  values obtained were very different, reaching a higher maximum velocity with DDB as substrate. In addition, it is possible to observe that the  $K_M$  values are very similar, which means that the affinity of malate for MQO is similar whether the second substrate is DMN or DDB. Comparing the  $V_{max}$  values obtained in the case of MQO from *E. coli* it is possible to observe that the maximum velocity that the protein can reach is dependent on which quinone is used.

#### 4.2.5. Inhibition assays

An enzyme inhibitor is a molecule that can bind to the protein and decrease its activity. HQNO, a quinone analogue, was used to perform inhibition assays in order to understand the effect of this inhibitor in the activity of MQO 1 from *S. aureus*. These assays were done using different inhibitor concentrations and the obtained data are shown in Figure 4.19.

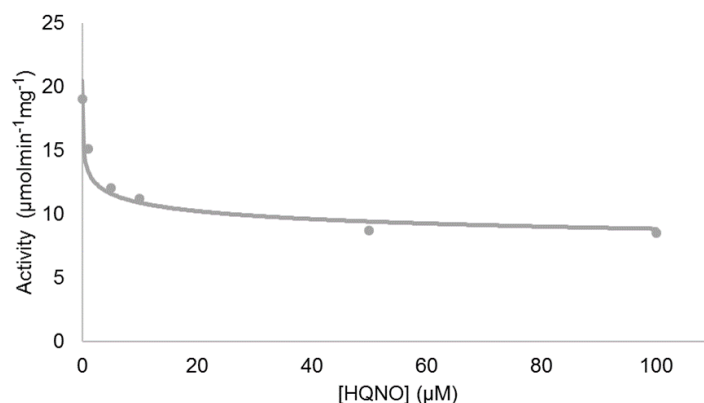


**Figure 4.19-** Steady-state analyses of the activity of MQO 1 from *S. aureus* in the presence of HQNO. Inhibition assays were performed in the presence of 3000  $\mu\text{M}$  malate, 100  $\mu\text{M}$  DMN, 125 nM MQO 1 from *S. aureus*, under anaerobic conditions, using scavenging system, at 37 °C in 50 mM potassium phosphate pH 7, 10 % glycerol, 250 mM NaCl. The concentrations of HQNO tested were 0, 1, 5, 10, 50 and 100  $\mu\text{M}$ .

Figure 4.19 shows a decrease in the activity of MQO 1 from *S. aureus* with the increase of HQNO concentration, meaning that HQNO is an inhibitor of this protein. In addition, the catalytic activity of the enzyme is only affected by about half by the presence of the inhibitor. The inhibition constant ( $K_i$ ) was determined using the obtained data and the equation  $V_0^i = V_0^{max} \frac{(1 + \beta \frac{[I]}{K_i})}{(1 + \frac{[I]}{K_i})}$  and the value obtained was  $5.1 \pm 0.8 \mu\text{M}$ .

Considering this result, we decided to investigate how the inhibitor affects the kinetic parameters of the MQO 1 from *S. aureus*. For that, two concentrations of HQNO were selected, 10 and 20  $\mu\text{M}$  and the

steady-state kinetic assays for MQO 1 were repeated but this time in the presence of each one of HQNO concentrations, Figure 4.20.

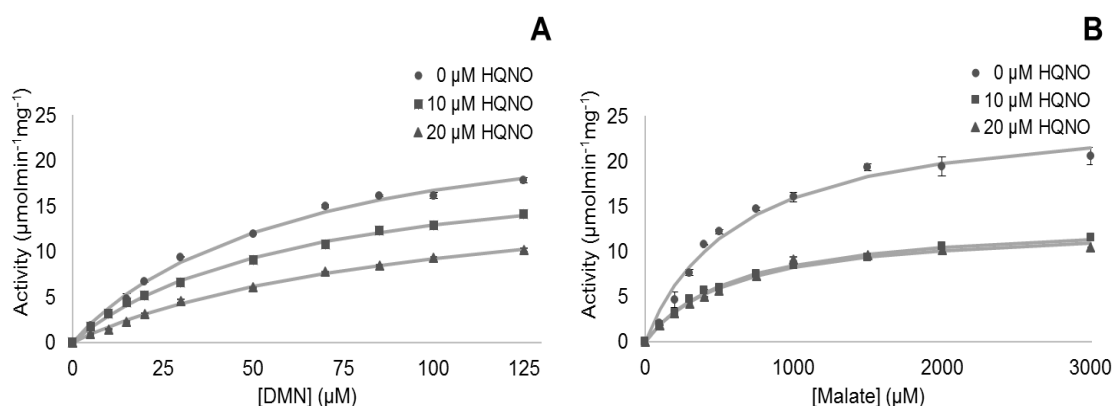


**Figure 4.20-** Steady-state analyses of the activity of MQO 1 from *S. aureus* in the presence of two different concentrations of HQNO. Malate:quinone oxidoreductase activity as function of the concentration of DMN (**A**) or malate (**B**) using 125 nM MQO 1 from *S. aureus* in the presence of 0  $\mu\text{M}$  (circles), 10  $\mu\text{M}$  (squares) or 20  $\mu\text{M}$  (triangles) of HQNO; All assays were performed under anaerobic conditions, using scavenging system, at 37  $^{\circ}\text{C}$  in 50 mM potassium phosphate pH 7, 10 % glycerol, 250 mM NaCl.

In Figure 4.20, it is possible to observe a dependency on the substrate, by increasing the concentration of the substrates, there is an increase on the activity of the protein until it reaches the maximum velocity. The characteristic Michaelis-Menten's behavior already observed in the absence of the inhibitor is also observed in its presence.

Figure 4.20-A, that represents malate:quinone oxidoreductase activity as function of the concentration of DMN, shows that the increase of the inhibitor concentration causes a gradual decrease in protein activity. Whereas in Figure 4.20-B, presenting malate:quinone oxidoreductase activity as function of the concentration of malate, the addition of the inhibitor causes a strong decrease to half of the protein activity but there is no difference in protein activity between the two HQNO concentrations used.

From the data obtained and using the Michaelis-Menten equation, it was possible to calculate the kinetic parameters for MQO 1 in each condition and the obtained results are shown in Table 4.4 for DMN and Table 4.5 for malate.

**Table 4.4-** Kinetic parameters of MQO 1 from *S. aureus* obtained for DMN in the presence of 0, 10 and 20  $\mu\text{M}$  HQNO. Determination of kinetic parameters was done using the Michaelis-Menten equation.

	DMN		
	0 $\mu\text{M}$ HQNO	10 $\mu\text{M}$ HQNO	20 $\mu\text{M}$ HQNO
$K_M$ ( $\mu\text{M}$ )	$61.4 \pm 3.8$	$62.7 \pm 5.9$ (+ 2 %)	$99.1 \pm 5.0$ (+ 62 %)
$V_{\max}$ ( $\mu\text{mol min}^{-1}\text{mg}^{-1}$ )	$27.0 \pm 0.6$	$21.0 \pm 0.9$ (- 22 %)	$18.4 \pm 0.5$ (- 32 %)

**Table 4.5**-Kinetic parameters of MQO 1 from *S. aureus* obtained for malate in the presence of 0, 10 and 20  $\mu\text{M}$  HQNO. Determination of kinetic parameters was done using the Michaelis-Menten equation.

	Malic acid		
	0 $\mu\text{M}$ HQNO	10 $\mu\text{M}$ HQNO	20 $\mu\text{M}$ HQNO
$K_M$ ( $\mu\text{M}$ )	$646.5 \pm 9.0$	$615.8 \pm 39.8$ (- 5 %)	$609.2 \pm 3.4$ (- 6 %)
$V_{\max}$ ( $\mu\text{mol min}^{-1}\text{mg}^{-1}$ )	$27.0 \pm 0.6$	$13.7 \pm 0.2$ (- 49 %)	$13.2 \pm 0.1$ (- 51 %)

The  $V_{\max}$  values listed in Tables 4.4. and 4.5 confirm the observation on Figure 4.20 that in the case of DMN the increase of the inhibitor's concentration causes a gradual decrease in the maximum velocity, while in the case of malate, adding the inhibitor causes a stronger decrease in the maximum velocity, but there is no difference on the  $V_{\max}$  when the concentration of the inhibitor increases from 10 to 20  $\mu\text{M}$ .

In addition, the obtained  $K_M$  values showed that the inhibitor seems to only affect the partial reaction with DMN. The  $K_M$  values for malate in the presence and absence of the inhibitor are very similar, the presence of the inhibitor translates into a 5 % decrease, which means that the affinity of the protein to this substrate is not affected by the presence of HQNO. On the other hand, the  $K_M$  values for DMN increase with the increasing of the inhibitor concentration. The presence of 20  $\mu\text{M}$  of inhibitor causes an increase in the  $K_M$  value by 62 %, meaning that HQNO affects the affinity of the protein to the quinone. Concluding, the  $V_{\max}$  values of both substrates showed that the inhibitor decreases the activity of the protein, although in the case of DMN it is a gradual decrease (22 % and 32 %) and in the case of malate it is a stronger decrease (49 % and 51 %). In addition, the presence of HQNO seems to only affect the affinity of the protein to DMN, since the  $K_M$  value of malate in the presence of 20  $\mu\text{M}$  of inhibitor decreases by 6 % and in the case of DMN it increases by 62 %.

#### 4.2.6. Fluorescence substrate binding studies

There are different techniques to investigate protein-substrate interaction, such as Saturation Transfer Difference Spectroscopy and Isothermal Titration Calorimetry. In this work, we used a fluorescence quenching methodology.

Fluorescence studies provide information about the changes in fluorescence of specific protein residues or cofactors, such as tryptophan residues, caused by environmental changes due to the presence of a molecule that interacts with the protein. Since MQO 1 from *S. aureus* has six tryptophan residues in its sequence and tryptophan when excited at 280 nm has a fluorescence emission spectrum with a maximum around 330 nm, it was possible to investigate the protein-ligand interaction using fluorescence quenching studies.

For these studies, three independent titrations were done with DMN ranging from 0 to 100  $\mu\text{M}$  and for oxaloacetate using concentrations from 100 to 3000  $\mu\text{M}$  (Figure 4.21). In these experiments we used oxaloacetate instead of malate to avoid protein reduction by the malate, and to only observe protein-ligand interaction and not the consequence of oxidoreduction reactions. The obtained data were

analyzed by the equation  $\Delta F = \frac{\Delta F_{\max} \times [S]}{K_D + [S]}$  in order to determine the substrate-enzyme dissociation constants ( $K_D$ ) of DMN and oxaloacetate.

In addition, we aimed to investigate the effect of HQNO in both DMN and oxaloacetate interactions, but for that it was necessary to investigate the interaction of the protein alone with HQNO. In order to know how the inhibitor interacts with the protein, three independent titrations of HQNO ranging from 0 to 125  $\mu\text{M}$  were done and the obtained data were also fitted using the same equation as above (Figure 4.21). Finally, in order to investigate if the interaction of both substrates, DMN and oxaloacetate, with the protein, was affected by the presence of the inhibitor, the titrations of DMN and oxaloacetate were repeated but this time in the presence of 200  $\mu\text{M}$  HQNO (Figure 4.21).

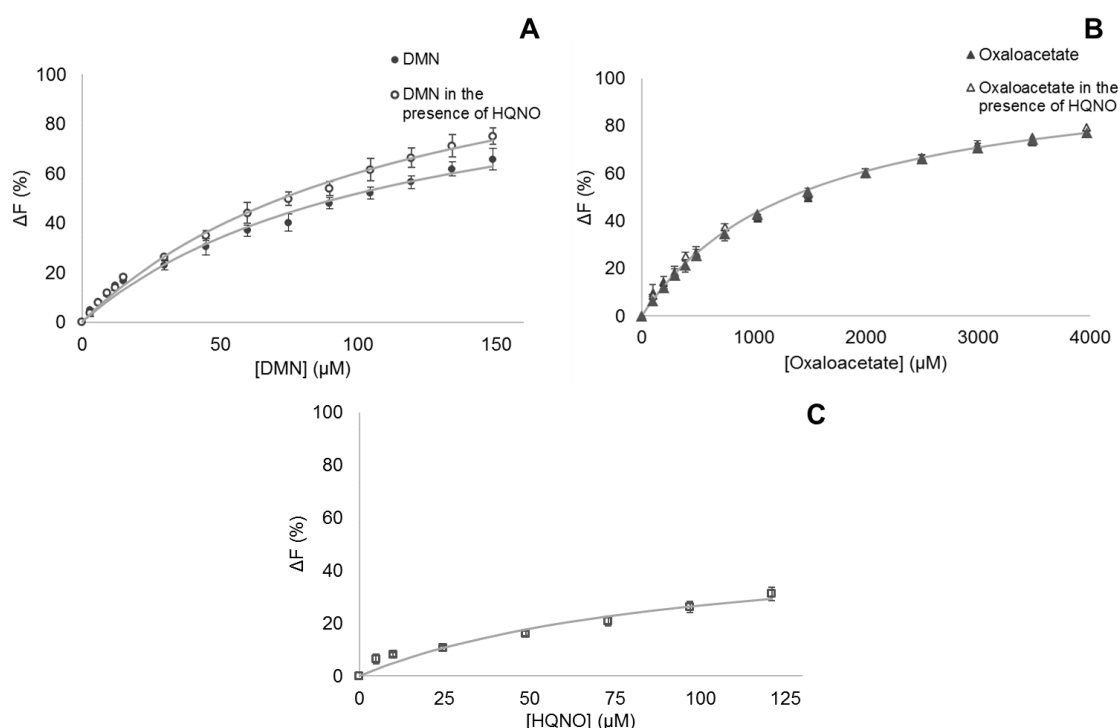


**Figure 4.21-** Protein-substrate interaction studies. **A-** Change in fluorescence emission at 330 nm with excitation at 295 nm of MQO 1 from *S. aureus* by sequential addition of DMN (closed circles) and in the presence of HQNO (open circles); **B-** Change in the fluorescence emission at 330 nm with excitation at 280 nm of MQO 1 from *S. aureus* by sequential addition of oxaloacetate (closed triangles) and in the presence of HQNO (open triangles). **C-** Change in the fluorescence emission at 330 nm with excitation at 280 nm of MQO 1 from *S. aureus* by sequential addition of HQNO (open squares). The solid lines were obtained by fitting the data using the equation  $\Delta F = \frac{\Delta F_{\max} \times [S]}{K_D + [S]}$ .

The substrate-enzyme dissociation constants ( $K_D$ ) were determined according to the equation mentioned above and the values are presented in Table 4.6.

**Table 4.6-** Substrate-enzyme dissociation constants of MQO 1 from *S. aureus* determined for both substrates in the absence and in the presence of HQNO.

	DMN	DMN in the presence of HQNO	Oxaloacetate	Oxaloacetate in the presence of HQNO
$K_D$ ( $\mu$ M)	$111.8 \pm 8.1$	$119.1 \pm 5.7$	$1572.2 \pm 256.4$	$1448.6 \pm 90.0$

In Figure 4.21, it is possible to observe that the maximum decrease in tryptophan fluorescence ( $\Delta F_{\max}$ ) in the presence of DMN and oxaloacetate, when titrated independently, is around 65 % and 75 %, respectively, while the  $\Delta F_{\max}$  of HQNO is approximately 30 %. These different values of  $\Delta F_{\max}$  indicate that the environment of the tryptophan residues is perturbed differently by the DMN, oxaloacetate and HQNO. In the case of the titrations in the presence of HQNO, it is possible to observe that the interaction of oxaloacetate with MQO has exactly the same behavior as the one in the absence of HQNO, meaning that the environment of the tryptophan residues involved in the interaction of the protein with oxaloacetate is not perturbed by the presence of HQNO. While in the case of the DMN titration, the curve obtained in the presence of HQNO shows slight differences from, which we can suppose that the environment of the tryptophan residues that are involved in the interaction of the protein with DMN is perturbed in the presence of the inhibitor.

Considering the obtained  $K_D$  values represented in Table 4.6, we can observe that they are very similar both in the presence and absence of the inhibitor, which implies that HQNO seems to not strongly affect the interaction of the substrates with MQO. Combining these  $K_D$  values with the results shown in Figure 4.21, we can conclude that the environment of the tryptophan residues is perturbed by HQNO alone, but there are no changes when the inhibitor is combined with one of the substrates, the  $K_D$  values being the same. This result is also in agreement with the fact that HQNO only inhibits half of the activity of MQO 1 from *S. aureus*, proving not to be a strong inhibitor and showing that new assay trials with other inhibitors are needed in the future.





## 5. Conclusion

MQOs are proteins widely distributed in the three domains of life but absent in humans. We aimed to investigate MQOs from different pathogenic organisms due to their threat to human health. In this study, MQOs from *Staphylococcus aureus*, *Escherichia coli*, *Helicobacter pylori* and *Plasmodium falciparum* were selected, since these proteins are considered potential drug targets to produce pharmaceuticals against these pathogenic organisms. We aimed to biochemically and functionally characterize these proteins. In addition, since the selected organisms synthesize different quinones depending on the growth conditions (aerobic or anaerobic) it was also our objective to study the effect of different quinones in the activity of the MQOs.

The expression tests allowed us to find the best condition for the expression of the four MQOs and three of them, MQO 1 and 2 from *S. aureus* and MQO from *E. coli*, were successfully purified. The purified samples showed a characteristic flavin UV-Visible spectrum and we could observe a band with the respective expected size in the SDS-PAGE gel. MQO 1 from *S. aureus* and MQO from *E. coli* showed malate:quinone oxidoreductase activity and mass spectrometry analysis of MQO 1 from *S. aureus* confirmed its identity. We were unable to get mass spectrometry data from the MQO from *E. coli* and MQO 2 from *S. aureus*. The isolated MQO 2 from *S. aureus* did not present malate:quinone oxidoreductase activity in the conditions tested, so it is necessary to determine which are the best conditions to the protein being active. Nevertheless, the protein identity must still be confirmed.

The pH profile of MQO from *E. coli* revealed that the optimal pH of the protein activity is at pH 7, which is in agreement with the cytoplasmic pH of *E. coli*. The steady-state kinetic studies performed with two different quinones, DMN and DDB, showed that the protein has higher activity when DDB is the electron acceptor, meaning that the purified MQO from *E. coli* prefers DDB instead of DMN, which agrees with the fact that the growth was performed under aerobic conditions and DDB is synthesized in those conditions.

MQO 1 from *S. aureus* was identified by mass spectrometry, and the prosthetic group FAD was detected by reverse chromatography. In addition, this protein showed to be redox active and the native PAGE gel revealed that MQO 1 from *S. aureus* is mainly a monomer in solution. The enzyme presented a characteristic Michaelis-Menten behavior toward the two substrates, requiring more malate than DMN to reach the maximum velocity. The activity of this protein is affected by HQNO, a quinone inhibitor, and the inhibition assays showed that the presence of this inhibitor decreases the affinity of the protein for DMN, while the affinity to malate is not affected. Fluorescence spectroscopic data revealed that DMN, oxaloacetate and HQNO perturb differently the environment of the tryptophan residues of MQOs. In addition, it was observed that HQNO alone perturbs the environment of the tryptophan residues, but when the substrates were titrated in the presence of this inhibitor there are no changes in the environment of the tryptophan residues, suggesting that HQNO does not affect tightly the interaction of both substrates with MQO.

This work provides a thorough investigation of MQOs and opens new perspectives for future studies in this field. In the future, Fast Kinetic assays can be performed in order to determine the rate constants of the two half-reactions (the reduction of the quinone to quinol and the oxidation of the malate to oxaloacetate) and investigate which half-reaction is the rate limiting step. Since HQNO showed to be a weak inhibitor of MQO, the screening of new inhibitors can also be performed in order to explore stronger inhibitors. Whereas the structure of a protein is associated with its function, obtaining the crystal structure of MQOs by X-ray crystallography will be a very important requirement for the investigation of these proteins.

Since MQOs have a crucial role on the metabolism of different pathogenic organisms, it is our goal to deepen the investigation of these proteins in functional and structural terms.

## 6. References

1. Devlin, T. M. (1997) *Textbook of biochemistry with clinical correlations* (4<sup>th</sup> ed.). New York: Wiley-Liss.
2. Nelson, M. C. and Cox, M. M. (2005) *Lehninger Principles of Biochemistry* (4<sup>th</sup> ed.). New York: W.H.Freeman.
3. Boiteux, A. and Hess, B. (1981) Design of glycolysis. *Philos Trans R Soc Lond B Biol Sci* 293 (1063), 5-22.
4. Fernie, A. R., Carrari, F. and Sweetlove, L. J. (2004) Respiratory metabolism: Glycolysis, the TCA cycle and mitochondrial electron transport. *Curr Opin Plant Biol* 7 (3), 254-261.
5. Hartuti, E.D., et al. (2018) Biochemical studies of membrane bound *Plasmodium falciparum* mitochondrial L-malate:quinone oxidoreductase, a potential drug target. *Biochim Biophys Acta - Bioenerg* 1859 (3),191-200.
6. Van der Rest, M. E. , Frank, C. and Molenaar, D. (2000) Functions of the membrane-associated and cytoplasmic malate dehydrogenases in the citric acid cycle of *Escherichia coli*. *J Bacteriol* 182 (24), 6892-6899.
7. Kather, B., et al. (2000) Another unusual type of citric acid cycle enzyme in *Helicobacter pylori*: The malate:quinone oxidoreductase. *J Bacteriol* 182 (11), 3204-3209.
8. Molenaar, D., van der Rest, M. E. and Petrovic, S. (1998) Biochemical and genetic characterization of the membrane-associated malate dehydrogenase (acceptor) from *Corynebacterium glutamicum*. *Eur J Biochem* 254 (2), 395-403.
9. Kabashima, Y., et al. (2013) Purification and characterization of malate:quinone oxidoreductase from thermophilic *Bacillus* sp. PS3. *J Bioenerg Biomembr* 45 (1-2), 131-136.
10. Baynes, J. W., Dominiczak, M. H. (2014) *Medical Biochemistry* (4<sup>th</sup> ed.). Philadelphia: Sauders.
11. Ke, H., et al. (2015) Genetic investigation of tricarboxylic acid metabolism during the *Plasmodium falciparum* life cycle. *Cell Rep* 11 (1), 164-74.
12. Sousa, J. S., D'Imprima, E. and Vonck, J. (2018) Mitochondrial Respiratory Chain Complexes. *Subcell Biochem* 87, 167-227.
13. Sazanov, L. A. (2007) Respiratory complex I: Mechanistic and structural insights provided by the crystal structure of the hydrophilic domain. *Biochemistry* 46 (9), 2275-88.
14. Sazanov, L. A. (2014) The mechanism of coupling between electron transfer and proton translocation in respiratory complex I, *J Bioenerg Biomembr* 46 (4), 247-253.
15. Cecchini, G. (2003) Function and Structure of Complex II of the Respiratory Chain. *Annu Rev Biochem* 72, 77-109.
16. Marreiros, B.C., et al. (2016) Exploring membrane respiratory chains. *Biochim Biophys Acta - Bioenerg* 1857 (8), 1039-1067.
17. Allen, K. N., et al. (2019) Monotopic Membrane Proteins Join the Fold. *Trends Biochem Sci* 44 (1), 7-20.

18. Wang, X., et al. (2019) Identification of *Plasmodium falciparum* Mitochondrial Malate: Quinone Oxidoreductase Inhibitors from the Pathogen Box. *Genes (Basel)* 10 (6), 1-11.
19. COHN, D. V. (1958) The enzymatic formation of oxalacetic acid by nonpyridine nucleotide malic dehydrogenase of *Micrococcus lysodeikticus*. *J Biol Chem* 2, 299-304.
20. Aliverti, A., Curti, B. and Vanoni, M. A. (1999) Identifying and quantitating FAD and FMN in simple and in iron-sulfur-containing flavoproteins. *Methods Mol Biol* 182 (11), 9-23.
21. Wallace, B. J. and Young, I. G. (1977) Role of Quinones in Electron Transport To Oxygen and Nitrate in *Escherichia Coli*. Studies with a ubiA-menA- double quinone mutant. *Biochim Biophys Acta* 461 (1), 84-100.
22. Wiley, J. (2007) "Methicillin-Resistant *Staphylococcus aureus*", in *Handbook of Current and Emerging Drug Therapies* 3 (5). New Jersey: Wiley Technology, 720-767.
23. Kumar, S. (2012) *Textbook of Microbiology*. New Delhi: Jaypee Brothers Medical Publishers.
24. Fuchs, S., et al. (2007) Anaerobic gene expression in *Staphylococcus aureus*. *J Bacteriol* 189 (11), 4275-4289.
25. Chambers, H. F. (2001) The Changing Epidemiology of *Staphylococcus aureus* ?, *Emerging Infectious Diseases* 7 (2), 178-182.
26. Watkins, R. R., David, M. Z., and Salata, R. A. (2012) Current concepts on the virulence mechanisms of methicillin-resistant *Staphylococcus aureus*. *J Med Microbiol* 61 (9), 1179-1193.
27. Fuller, J. R., et al. (2011) Identification of a lactate-quinone oxidoreductase in *Staphylococcus aureus* that is essential for virulence. *Front Cell Infect Microbiol* 1 (19), 1-15.
28. Lin, Y.C., et al. (2019) Emergence of an *Escherichia coli* strain co-harboring mcr-1 and bla NDM-9 from a urinary tract infection in Taiwan. *J Glob Antimicrob Resist* 16, 286-290.
29. Farhadkhani, M., et al. (2019) Potential transmission sources of *Helicobacter pylori* infection: Detection of *H. pylori* in various environmental samples. *J Environ Heal Sci Eng* 17 (1), 129-134.
30. Florens, L., et al. (2002) A proteomic view of the *Plasmodium falciparum* life cycle. *Nature* 419 (6926), 520-526.
31. Froger, A. and Hall, J. E. (2007) Transformation of Plasmid DNA into E. Coli using the heat shock method, *J Vis Exp* 6, 253.
32. Thermo Scientific. (2011) User Guide: Pierce BCA Protein Assay Kit. *Pierce Biotechnol*, 1-7.
33. Schmid, F. (2001) Biological Macromolecules : UV-Visible Spectrophotometry. *Encyclopedia of Life Sciences*, 1-4.
34. Arshad, A., et al. (2015) A metagenomics-based metabolic model of nitrate-dependent anaerobic oxidation of methane by *Methanoperedens*-like Archaea. *Front Microbiol* 6 (1423), 1-14.
35. Matsuno, T., et al. (2009) Physiological role and redox properties of a small cytochrome c5, cytochrome c-552, from alkaliphile, *Pseudomonas alcaliphila* AL15-21T. *J Biosci Bioeng* 108 (6), 465-470.
36. Grimsley, G. R. and Pace, C. N. (2004) Spectrophotometric determination of protein concentration. *Curr Protoc protein Sci*.

37. Slonczewski, J. L., et al. (2009) Cytoplasmic PH Measurement and Homeostasis in Bacteria and Archaea. *Adv Microb Physiol* 55, 1-79.
38. Wilks, J. C. and Slonczewski, J. L. (2007) pH of the cytoplasm and periplasm of *Escherichia coli*: Rapid measurement by green fluorescent protein fluorimetry. *J Bacteriol* 189 (15), 5601-5607.



## 7. Appendix

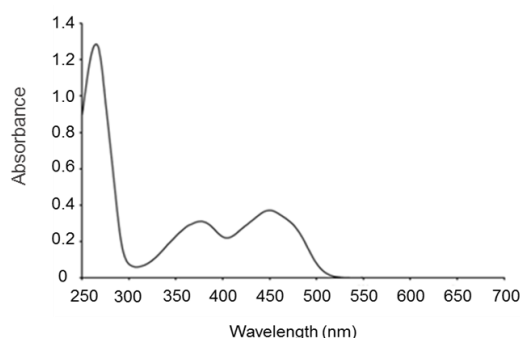


**Figure 7.1-** Flavin adenine nucleotide UV-Visible spectrum.

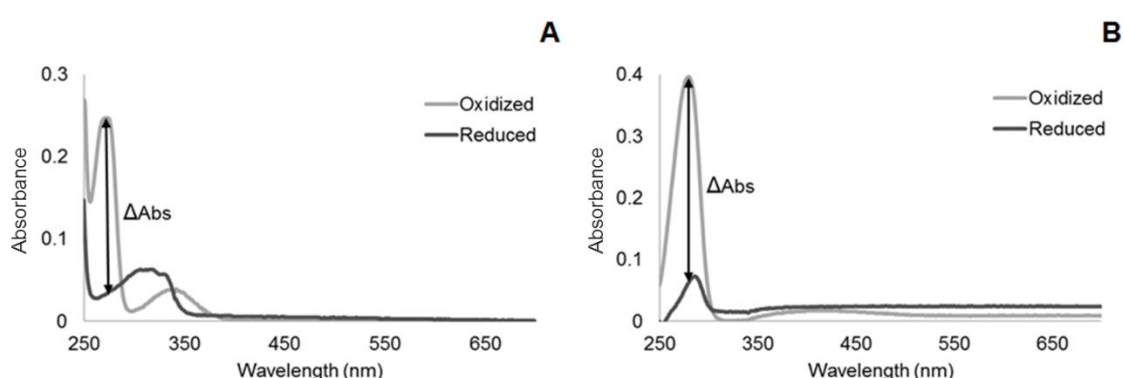


**Figure 7.2-** UV-Visible spectra of oxidized (light grey) and reduced (dark grey) DMN (A) or DDB (B) with  $\text{NaBH}_4$ . A- The  $\Delta\text{Abs}$  is higher at 270 nm. B- The  $\Delta\text{Abs}$  is higher at 278 nm.  $\Delta\text{Abs}$  represents the difference in the absorbance between oxidized and reduced spectra. Spectra obtained in an anaerobic chamber, using 20  $\mu\text{M}$  or 75  $\mu\text{M}$  of DMN or DDB, respectively, and 2 mM of  $\text{NaBH}_4$ .

**Table 7.1-** Compositions of the media used to perform expression tests and cell growth.

Media	Reagent (Brand)	Quantity
Luria Bertani Agar (LA) (1000 mL)	Yeast Extract (VWR)	5 g
	NaCl (Panreac)	10 g
	Tryptone (VWR)	10 g
	Agar (VWR)	10 g
Luria Bertani (LB) (1000 mL)	Yeast Extract (VWR)	5 g
	NaCl (Panreac)	10 g
	Tryptone (VWR)	10 g
Yeast Extract and Tryptone (2YT) (1000 mL)	Yeast Extract (VWR)	10 g
	NaCl (Panreac)	5 g
	Tryptone (VWR)	16 g
Terrific Broth (TB) (1000 mL)	$\text{KH}_2\text{PO}_4$ (VWR)	2.314 g
	$\text{K}_2\text{HPO}_4$ (VWR)	12.541 g
	Tryptone (VWR)	10.8 g
	Yeast Extract (VWR)	21.6 g
	Glycerol (VWR)	4 mL

**Table 7.2-** Composition of the solutions used in SDS-PAGE and NATIVE PAGE gels.

	Solution	Reagent (Brand)	Quantity
SDS-PAGE gel	Loading Buffer (9 mL)	Tris-HCl (Panreac)	4 mL
		SDS (Bio-Rad)	0.8 g
		Bromophenol Blue (Sigma- Aldrich)	0.04 g
		Glycerol (VWR)	4.6 mL
		$\beta$ -mercaptoethanol (Sigma- Aldrich)	0.4 mL
		Urea (Panreac)	3.84 g
	Coomassie (310 mL)	Brilliant Blue (Sigma- Aldrich)	0.5 g
		Methanol (Sigma- Aldrich)	250 mL
		Acetic Glacial Acid (Sigma- Aldrich)	50 mL
	Distaining Solution (1000 mL)	Ethanol (LaborSpirit)	400 mL
		Acetic Glacial Acid (Sigma- Aldrich)	100 mL
	Running Buffer pH 8.3 (2000 mL)	Tris-HCl (Panreac)	6 g
		Glycine (Carl Roth)	40 g
		SDS (Bio-Rad)	2 g
	Resolving gel Buffer pH 8.8 (100 mL)	Tris-HCl (Panreac)	18.2 g
		SDS (Bio-Rad)	0.3 g
	Stacking gel Buffer pH 6.8 (100 mL)	Tris-HCl (Panreac)	6 g
		SDS (Bio-Rad)	0.4 g
NATIVE PAGE gel	Resolving gel 15 %	H <sub>2</sub> O	2.3 mL
		Resolving gel Buffer pH 8.8	2.6 mL
		Acrylamide (Sigma- Aldrich)	5 mL
		TEMED (Sigma- Aldrich)	0.004 mL
		APS (Carl Roth)	0.1 mL
	Stacking gel 15 %	H <sub>2</sub> O	1.4 mL
		Stacking gel Buffer pH 6.8	0.27 mL
		Acrylamide (Sigma- Aldrich)	0.33 mL
		TEMED (Sigma- Aldrich)	0.002 mL
		APS (Carl Roth)	0.02 mL
	Anode Running Buffer pH 6.8 (20x) (1000 mL)	BisTris (Sigma- Aldrich)	209.2 g
		Tricine (Sigma- Aldrich)	179.2 g
	Anode Running Buffer (1x) (1000 mL)	Anode Running Buffer pH 6.8 (20x)	50 mL
	Cathode Running Buffer (20x) (250 mL)	Coomassie G-250 (Sigma- Aldrich)	1 g
	Cathode Running Buffer (1x) (200 mL)	Anode Running Buffer pH 6.8 (20x)	10 mL
		Cathode Running Buffer (20x)	10 mL
	Sample Buffer (4x) (10 mL)	BisTris (Sigma- Aldrich)	0.418 g
		6 N HCl (Fluka)	0.107 mL
		Glycerol (VWR)	4 g
		NaCl (Panreac)	0.117 g
		Ponceau S (Sigma- Aldrich)	0.0004 g
	G-250 (10 mL)	Coomassie G-250 (Sigma- Aldrich)	0.5 g



## Mass Spectrometry Unit

Assay Report: UniMS101/19



### Protein sequence coverage:

Sample MR1 SA

*{MATRIX}*  
*{SCIENCE}* MASCOT SEARCH RESULTS

### PROTEIN VIEW

Match to: T1YB17\_STAAU Score: 335 Expect: 3.2e-029  
Probable malate:quinone oxidoreductase OS=Staphylococcus aureus subsp.  
aureus CN1 OX=1193576 GN=mgo PE=3 SV=1

Nominal mass ( $M_r$ ): 56950; Calculated pI value: 6.59

Variable modifications: Carbamidomethyl (C), Deamidated (NQ), Gln->pyro-Glu  
(N-term Q), Oxidation (M)

Cleavage by Trypsin: cuts C-term side of KR unless next residue is P  
Sequence Coverage: 49%

Matched peptides shown in **Bold Red**

```

1  MSYFSNVPLF ILKRGTVFVM TTQHSKTDVI LIGGGIMSAT LGTLLKELSP
51 EKNIKVFEKL AQPGEESNV WNNAGTGHS A LCELNYTKEG KDGTVDCSKA
101 IKINEQQYQIS KQFWAYLVKT GQLDNPDFI QAVPHMSFVI GMDNVAFIKS
151 RVATLKRSVL FEKMKLSQDE EEMKSWVPLM IEGRKSDEPI ALTYDETGTD
201 VNFGALTAKL FENLEQRGVG IQYKQNVLDI KKQKSGAWLV KVKDLSTNET
251 TTYESDFVFI GAGGASLPLL QKTGIQSKH IGGFPVSGLF LRCTNQEVID
301 RHHAKVYGKA AVGAPFMSVP HLDTRFVDGK RSLLEFSPFAG FSPKFLKTGS
351 HMDLIKSVKP NNIVTMLSAG IKEMSLTKYL VSQMLNSDE RMDDLRFVFP
401 NAKNEDWEVI TAGQRVQVIK DTEDSKGNLQ FGTEVITSDD GTLAALLGAS
451 PGASTAVDIM FDVLQRCYRD EFKGWEPKIK EMVPSFGYRL TDHEDLYHKI
501 NEEVTKYLQV K
    
```

**Figure 7.3-** Mass Spectrometry Unit Assay Report. Report of the analysis to the identification of the protein purified.

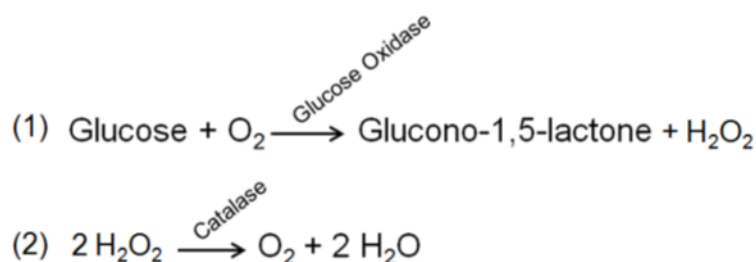


**Figure 7.4-** Reactions of Scavenging System. (1)- Glucose Oxidase consumes oxygen and glucose to form hydrogen peroxide. (2)- Catalase consumes the hydrogen peroxide formed in (1) and yielding molecular oxygen and water.

**Table 7.3-** Kinetic parameters of MQO 1 from *S. aureus* obtained for DMN and malate. Determination of kinetic parameters was done using the Michaelis-Menten equation.

	DMN	Malate
$K_M$ ( $\mu\text{M}$ )	$61.4 \pm 3.8$	$646.5 \pm 9.0$
$V_{\max}$ ( $\mu\text{mol min}^{-1}\text{mg}^{-1}$ )	$27.0 \pm 0.6$	$26.1 \pm 0.1$

**Table 7.4-** Kinetic parameters of MQO from *E. coli* obtained for DDB and DMN. Determination of kinetic parameters was done using the Michaelis-Menten equation.

	DDB	DMN
$K_M$ ( $\mu\text{M}$ )	$22.7 \pm 1.5$	$53.1 \pm 3.9$
$V_{\max}$ ( $\mu\text{mol min}^{-1}\text{mg}^{-1}$ )	$12.3 \pm 0.3$	$5.0 \pm 0.2$

**Table 7.5-** Kinetic parameters of MQO from *E. coli* obtained for malate using DDB and DMN. Determination of kinetic parameters was done using the Michaelis-Menten equation.

	DDB	DMN
$K_M$ ( $\mu\text{M}$ )	$202.1 \pm 9.9$	$242.0 \pm 21.4$
$V_{\max}$ ( $\mu\text{mol min}^{-1}\text{mg}^{-1}$ )	$11.6 \pm 0.0$	$5.1 \pm 0.2$